Eur. Phys. J. Plus (2017) **132**: 461
DOI 10.1140/epjp/i2017-11739-6

THE EUROPEAN PHYSICAL JOURNAL PLUS

Regular Article

Bifurcations and chaos of time delay Lorenz system with dimension 2n + 1

Gamal M. Mahmoud[1,a], Ayman A. Arafa[2,b], and Emad E. Mahmoud[2,3,c]

[1] Department of Mathematics, Faculty of Science, Assiut University, Assiut 71516, Egypt
[2] Department of Mathematics, Faculty of Science, Sohag University, Sohag 82524, Egypt
[3] Department of Mathematics, Faculty of Science, Taif University, Taif, Saudi Arabia

Received: 12 August 2017 / Revised: 1 October 2017
Published online: 7 November 2017 –

Abstract. The aim of this paper is to introduce a generalized form of the Lorenz system with time delay. Instead of considering each state variable of the Lorenz system belonging to $\mathbb{R}$, the paper considers two of them belonging to $\mathbb{R}^n$. Hence the Lorenz system has $(2n+1)$ dimension. This system appears in several applied sciences such as engineering, physics and networks. The stability of the trivial and nontrivial fixed points and the existence of Hopf bifurcations are studied analytically. Using the normal form theory and center manifold argument, the direction and the stability of the bifurcating periodic solutions are determined. Finally, numerical simulations are calculated to confirm our theoretical results. The paper concludes that the dynamics of this system are rich. Additionally, the values of the delay parameter at which chaotic and hyperchaotic solutions exist for different values of n using Lyapunov exponents and Kolmogorov-Sinai entropy are calculated numerically.

1 Introduction

In 1963, Lorenz introduced a particular simplified hydrodynamic flow problem [1]. This system is an approximation to the Navier-Stokes equations for the hydrodynamics problem given by Bénard. The following equations are derived from a model of fluid convection:

$$\begin{aligned}\dot{x}(t) &= \sigma\left(y(t) - x(t)\right),\\ \dot{y}(t) &= (\rho - z(t))x(t) - y(t),\\ \dot{z}(t) &= x(t)y(t) - \beta z(t),\end{aligned} \tag{1}$$

where the variable $x \in \mathbb{R}$ measures the rate of convection overturning, the variable $y \in \mathbb{R}$ measures the horizontal temperature variation and the variable $z \in \mathbb{R}$ measures the vertical temperature variation. The parameter σ is called the Prandtl number, ρ represents the Rayleigh number and β represents some physical proportions of the region under consideration. This system has chaotic attractors for wide ranges of values of the parameters, *e.g.* when $\sigma = 10$, $\beta = \frac{8}{3}$ and $\rho = 28$. Chaos has been studied extensively and developed with much interest by researchers. It has many applications in the biological systems, electrical engineering, networks, cryptography and image encryption. Thereafter, many chaotic systems have been appeared such as Chen, Rössler, Lü, and Chua systems [2–5].

As a generalization of the Lorenz system (1), Fowler *et al.* [6] introduced what is called a complex Lorenz system as

$$\begin{aligned}\dot{x}(t) &= \sigma\left(y(t) - x(t)\right),\\ \dot{y}(t) &= (\rho - z(t))x(t) - ay(t),\\ \dot{z}(t) &= \frac{1}{2}\left(x(t)\bar{y}(t) + \bar{x}(t)y(t)\right) - \beta z(t),\end{aligned} \tag{2}$$

[a] e-mail: gmahmoud@aun.edu.eg
[b] e-mail: ayman_math88@yahoo.com
[c] e-mail: emad_eluan@yahoo.com

where $x, y \in \mathbb{C}$ represent the electric field amplitude and the atomic polarization amplitude, respectively, and $z \in \mathbb{R}$ represents the population inversion in a ring laser system of two-level atoms. The complex parameters ρ and a are defined as $\rho = \rho_1 + i\rho_2$, $a = 1 - ie$, σ and β are real parameters, $i = \sqrt{-1}$ and an overbar denotes complex conjugate variable. Two decades later, Mahmoud *et al.* [7] investigated the basic properties and chaotic synchronization of the complex Lorenz model (2) by setting $\rho = \rho_1$, $a = 1$ as follows:

$$\begin{aligned}
\dot{x}(t) &= \sigma\left(y(t) - x(t)\right),\\
\dot{y}(t) &= (\rho_1 - z(t))x(t) - y(t),\\
\dot{z}(t) &= \frac{1}{2}\left(x(t)\bar{y}(t) + \bar{x}(t)y(t)\right) - \beta z(t),
\end{aligned} \tag{3}$$

where $x, y \in \mathbb{C}$, $z \in \mathbb{R}, \sigma, \rho$ and $\beta \in \mathbb{R}^+$. In fact, many systems which include complex and real variables have played an important role in many real applications, such as rotor dynamics [8], problems of laser physics [9], optical systems [10], and disk dynamos [11].

The time delay system is a system which the rate of variation of its states depends on past states. This system can be found in engineering [12], biology [13], as well as population dynamics [14]. Moreover, delays are strongly engaged in challenging areas of information and communication technologies, *e.g.* in stabilization of networked controlled systems and high-speed communication networks. It is well known that the existence of a delay in these systems inspires infinite dimensional. In particular, various complex phenomena have been arisen as a result of the existence of a time delay in a nonlinear system, such as bifurcation, multistability, chaos, hyperchaos, etc. On the other hand, since Mackay and Glass [15] studied chaos in time delay system, there are increasing interest in chaotic and hyperchaotic systems with delays [16–23].

Based on systems (1) and (3), this paper introduces and investigates a generalized form of $(2n+1)$ time delay Lorenz system as

$$\begin{aligned}
\dot{\boldsymbol{X}}(t) &= \sigma\left(\boldsymbol{Y}(t-\tau) - \boldsymbol{X}(t)\right),\\
\dot{\boldsymbol{Y}}(t) &= \rho\boldsymbol{X}(t) - \boldsymbol{Y}(t) - Z(t)\boldsymbol{X}(t),\\
\dot{Z}(t) &= \boldsymbol{X}^T(t)\boldsymbol{Y}(t) - \beta Z(t),
\end{aligned} \tag{4}$$

where $\boldsymbol{X} = (X_1, X_2, \ldots, X_n)^T \in \mathbb{R}^n$, $\boldsymbol{Y} = (Y_1, Y_2, \ldots, Y_n)^T \in \mathbb{R}^n$, $Z \in \mathbb{R}, \sigma, \rho$ and β are constant parameters, and $\tau \geq 0$ is a constant time delay. As a result of the presence of τ, system (4) has rich dynamics that do not exist in the corresponding system without delay.

Remark 1. For the case $n = 1$ and $\tau = 0$ we get Lorenz system (1).

Remark 2. If $n = 2$ and $\tau = 0$ system (4) becomes complex Lorenz system (3).

The importance of this system is that it can be used in many applications, including secure communications, and networks. Thus, the paper scrutinizes the local stability of system (4). Based on the distribution of eigenvalues of transcendental characteristic equation, some general stability criteria involving the system parameters are derived. Using the method stated by Hassard *et al.* [24], the validity of all conditions driving to a Hopf bifurcation for system (4) is demonstrated. Finally, chaos is confirmed by computing Lyapunov exponents and Kolmogorov-Sinai entropy of system (4) with different values of n.

The paper is organized as follows. In sect. 2, the fixed points and their stability of system (4) are calculated. The existence of Hopf bifurcation is studied analytically. In sect. 3, the approach introduced by Hassard *et al.* [24] is applied to compute the coefficients that determine the nature of the bifurcation and its stability. In sect. 4, some numerical simulations are performed, in order to justify the theoretical analysis of sects. 2 and 3. In sect. 5, the Lyapunov exponents and Kolmogorov-Sinai (KS) entropy are calculated for system (4) with different values of n. The values of the parameter τ at which, chaotic and hyperchaotic attractors of different orders exist are calculated numerically for $n = 2, 3, 10$. In sect. 6, the results are concluded and future works are indicated.

2 Dynamics of system (4)

In this section, the basic properties of system (4) are investigated. The fixed points can be obtained by setting $\dot{\boldsymbol{X}} = \boldsymbol{0}$, $\dot{\boldsymbol{Y}} = \boldsymbol{0}$, $\dot{Z} = 0$ and $\boldsymbol{Y}(t-\tau) = \boldsymbol{Y}(t)$, so system (4) has three fixed points:

$$\begin{aligned}
F_0 &= (0, 0, \ldots, 0) \in \mathbb{R}^{2n+1},\\
F_n^{\pm} &= \left(\pm\sqrt{\beta(\rho-1) - \sum_{l=2}^{n} X_l^{*2}}, X_2^*, \ldots, X_n^*, \pm\sqrt{\beta(\rho-1) - \sum_{l=2}^{n} X_l^{*2}}, X_2^*, \ldots, X_n^*, \rho - 1\right).
\end{aligned} \tag{5}$$

If $n = 1$, system (4) has three different fixed points [1]:

$$F_0 = (0, 0, 0), \qquad F_1^{\pm} = \left(\pm\sqrt{\beta(\rho-1)}, \pm\sqrt{\beta(\rho-1)}, \rho - 1\right).$$

When $n = 2$, it has an isolated fixed point $F_0 = (0, 0, 0, 0, 0)$ and a whole circle of equilibria which can be written as $(\pm\sqrt{\beta(\rho-1) - X_2^{*2}}, X_2^*, \pm\sqrt{\beta(\rho-1) - X_2^{*2}}, X_2^*, \rho - 1)$ [7].

2.1 The stability of $\mathbf{F_0}$

Now, the stability of the trivial fixed point F_0 are studied and investigated. The linearization of system (4) at F_0 is

$$\begin{aligned} \dot{\boldsymbol{X}}(t) &= \sigma\left(\boldsymbol{Y}(t-\tau) - \boldsymbol{X}(t)\right), \\ \dot{\boldsymbol{Y}}(t) &= \rho\boldsymbol{X}(t) - \boldsymbol{Y}(t), \\ \dot{Z}(t) &= -\beta Z(t). \end{aligned} \tag{6}$$

The associated characteristic equation of system (6) is

$$\det\begin{pmatrix} (-\sigma-\lambda)\boldsymbol{I}_n & \sigma e^{-\lambda\tau}\boldsymbol{I}_n & \mathbf{0} \\ \rho\boldsymbol{I}_n & (-1-\lambda)\boldsymbol{I}_n & \mathbf{0} \\ \mathbf{0}^T & \mathbf{0}^T & -\beta-\lambda \end{pmatrix} = 0,$$

where $\boldsymbol{I}_n$ is the $(n \times n)$ identity matrix and $\mathbf{0} = (0, 0, \ldots, 0)^T \in \mathbb{R}^n$. The characteristic equation of system (6) at F_0 is

$$(\lambda + \beta)\left(\lambda^2 + (\sigma+1)\lambda + \sigma - \rho\sigma e^{-\lambda\tau}\right)^n = 0. \tag{7}$$

Clearly, eq. (7) has a negative root $\lambda = -\beta$ for all $\tau \geq 0$. Thus, the second-degree transcendental polynomial equation is examined,

$$\lambda^2 + (\sigma+1)\lambda + \sigma - \rho\sigma e^{-\lambda\tau} = 0, \tag{8}$$

which can be written in general form as

$$\lambda^2 + a\lambda + b + ce^{-\lambda\tau} = 0, \tag{9}$$

where

$$a = \sigma + 1, \qquad b = \sigma, \qquad c = -\rho\sigma. \tag{10}$$

For $\tau = 0$, eq. (9) becomes

$$\lambda^2 + a\lambda + b + c = 0. \tag{11}$$

Equation (11) has negative real roots iff

$$a > 0 \quad \text{and} \quad b + c > 0. \tag{12}$$

For $\tau \neq 0$, and if $\lambda = i\omega$ $(\omega > 0)$ is a root of eq. (9), we obtain

$$-\omega^2 + ia\omega + b + c\left(\cos\omega\tau - i\sin\omega\tau\right) = 0.$$

By separating the real and imaginary parts, we get

$$\begin{cases} -\omega^2 + b = -c\cos\omega\tau, \\ a\omega = c\sin\omega\tau. \end{cases} \tag{13}$$

Adding up the squares of both equations of (13), we have

$$\omega^4 + (a^2 - 2b)\omega^2 + b^2 - c^2 = 0. \tag{14}$$

The roots of eq. (14) can be written as

$$\omega_{\pm}^2 = \frac{-(a^2-2b) \pm \sqrt{(a^2-2b)^2 - 4(b^2-c^2)}}{2}. \tag{15}$$

From eq. (10), it could be concluded that $a^2 - 2b > 0$. Consequently, eq. (14) does not have positive roots if one of the following conditions is satisfied:

$$b^2 - c^2 > 0 \quad \text{and} \quad \Delta^* = (a^2 - 2b)^2 - 4(b^2 - c^2) < 0. \tag{16}$$

That is, the characteristic equation (9) does not have purely imaginary roots, since, condition (12) ensures that all roots of eq. (11) have negative real parts.

Equation (15) shows that there is a unique positive solution ω_+^2 if

$$b^2 - c^2 < 0. \tag{17}$$

Then at

$$\tau_j = \frac{1}{\omega_+}\left(\arctan\left(\frac{a\omega_+}{\omega_+^2 - b}\right) + 2\pi j\right), \quad j = 0, 1, \ldots. \tag{18}$$

Moreover, eq. (9) has a simple pair of purely imaginary roots $\pm\omega_+$

$$\omega_+ = \sqrt{\frac{-(a^2 - 2b) \pm \sqrt{(a^2 - 2b)^2 - 4(b^2 - c^2)}}{2}}. \tag{19}$$

Now, we investigate the sign of

$$G = \text{sign}\left\{\frac{\mathrm{d}}{\mathrm{d}\tau} Re\,(\lambda(\tau))\right\}_{\tau=\tau_j},$$

where $\lambda(\tau) = v(\tau) \pm i\omega(\tau)$ are the roots of (9) near $\tau = \tau_j$ $(j = 0, 1, \ldots)$ satisfying $v(\tau_j) = 0$, $\omega(\tau_j) = \omega_+$. Here, we have the following transversality condition.

Lemma 1. *The following transversality condition*

$$\frac{\mathrm{d}}{\mathrm{d}\tau} Re\,(\lambda(\tau))_{\tau=\tau_j} > 0, \tag{20}$$

is satisfied.

Proof. Differentiating eq. (9) with respect to τ, we get

$$\frac{\mathrm{d}\lambda}{\mathrm{d}\tau}\left(2\lambda + a - c\tau e^{-\lambda\tau}\right) = c\lambda e^{-\lambda\tau}.$$

This gives

$$\begin{aligned}\left(\frac{\mathrm{d}\lambda}{\mathrm{d}\tau}\right)^{-1} &= \frac{(2\lambda + a)e^{\lambda\tau}}{c\lambda} - \frac{\tau}{\lambda}\\ &= \frac{-(2\lambda + a)}{\lambda\,(\lambda^2 + a\lambda + b)} - \frac{\tau}{\lambda}.\end{aligned}$$

Therefore

$$\begin{aligned}\text{sign}\left\{\frac{\mathrm{d}}{\mathrm{d}\tau} Re\,(\lambda(\tau))\right\}_{\lambda=i\omega_+} &= \text{sign}\left\{Re\left(\frac{\mathrm{d}\lambda(\tau)}{\mathrm{d}\tau}\right)^{-1}\right\}_{\lambda=i\omega_+}\\ &= \text{sign}\left\{Re\left(\frac{-(2\lambda + a)}{\lambda(\lambda^2 + a\lambda + b)}\right)_{\lambda=i\omega_+}\right\}\\ &= \text{sign}\left\{Re\left(\frac{-(2i\omega_+ + a)}{i\omega_+(-\omega_+^2 + ai\omega_+ + b)}\right)_{\lambda=i\omega_+}\right\}\\ &= \text{sign}\left\{\frac{a^2 - 2b + 2\omega_+^2}{a^2\omega_+^2 + (b - \omega_+^2)^2}\right\}.\end{aligned}$$

Since $a^2 - 2b > 0$, therefore

$$\frac{\mathrm{d}}{\mathrm{d}\tau} Re\,(\lambda(\tau))_{\lambda=i\omega_+} > 0.$$

From the above lemma, it could be concluded that if (17) holds, then (9) has at least one eigenvalue with strictly positive real part for $\tau > \tau_0$.

Theorem 1. *Let* τ_j *be defined by eq.* (18), $\beta > 0$ *and condition* (12) *holds:*

1) *The fixed point* F_0 *of system* (4) *is asymptotically stable for* $\tau \geq 0$ *if* (16) *satisfied. While, if* (17) *holds then* F_0 *is asymptotically stable for* $\tau \in [0, \tau_0)$ *and unstable for* $\tau > \tau_0$.
2) *Hopf bifurcation occurs when* $\tau = \tau_0$. *That is, a family of periodic solutions bifurcates from* F_0 *as* τ *passes through the critical value* τ_0.

2.2 The stability of $\mathbf{F_n^{\pm}}$

To study the stability of system (4) at the nontrivial fixed point $F_n^{\pm}$, the paper considers that the general form of the nontrivial fixed point is

$$F = (x_1^*, x_2^*, \ldots, x_n^*, y_1^*, y_2^*, \ldots, y_n^*, z^*).$$

Using the linear transform:

$$\begin{aligned} \mathbf{X}(t) &= \boldsymbol{x}(t) - \boldsymbol{x}^*, \\ \mathbf{Y}(t) &= \boldsymbol{y}(t) - \boldsymbol{y}^*, \\ Z(t) &= z(t) - z^*, \end{aligned} \tag{21}$$

system (4) becomes

$$\begin{aligned} \dot{\boldsymbol{x}}(t) &= \sigma \left(\boldsymbol{y}(t-\tau) - \boldsymbol{x}(t)\right), \\ \dot{\boldsymbol{y}}(t) &= \rho \boldsymbol{x}(t) - \boldsymbol{y}(t) - z^* \boldsymbol{x}(t) - \boldsymbol{x}^* z, \\ \dot{z}(t) &= (\boldsymbol{x}^*)^T \boldsymbol{y}(t) + \boldsymbol{x}^T(t) \boldsymbol{y}^* - \beta z(t). \end{aligned} \tag{22}$$

The associated characteristic equation of system (22) is

$$\begin{aligned} H(\lambda) = &\left(\lambda^2 + (\sigma+1)\lambda + \sigma - \sigma e^{-\lambda\tau}\right)^{n-1} \\ &\times \left(\lambda^3 + (1+\sigma+\beta)\lambda^2 + (\beta\rho + \sigma + \beta\sigma)\lambda + \sigma\rho\beta - \sigma(\lambda - \beta(\rho-2))e^{-\lambda\tau}\right) = 0. \end{aligned} \tag{23}$$

Denoting the two factors of $H(\lambda)$ by $H_1(\lambda)$ and $H_2(\lambda)$, respectively, we get

$$\begin{aligned} H_1(\lambda) &:= \left(\lambda^2 + (\sigma+1)\lambda + \sigma - \sigma e^{-\lambda\tau}\right)^{n-1}, \\ H_2(\lambda) &:= \lambda^3 + (1+\sigma+\beta)\lambda^2 + (\beta\rho + \sigma + \beta\sigma)\lambda + \sigma\rho\beta - \sigma(\lambda - \beta(\rho-2))e^{-\lambda\tau}. \end{aligned} \tag{24}$$

The following characteristic equation is considered:

$$H_1(\lambda) := \left(\lambda^2 + (\sigma+1)\lambda + \sigma - \sigma e^{-\lambda\tau}\right)^{n-1}, \tag{25}$$

which is similar to eq. (9) but with different coefficients, where

$$a = \sigma + 1, \qquad b = \sigma, \qquad c = -\sigma.$$

Now, we investigate the sign of real parts of the roots of (25). Clearly, for $\tau = 0$, $H_1(\lambda)$ does not have positive real parts. Also, for $\tau \neq 0$, if we set $\lambda = i\omega$, $\omega_\pm^2$ in eq. (15) does not have any positive roots. Therefore, the characteristic equation (25) does not have purely imaginary parts. So, it could be concluded that the equilibrium points $F_n^{\pm}$ of system (4) stable for all $\tau \geq 0$. Therefore, the other factor $H_2(\lambda)$ of the characteristic equation (23) is studied, which can be written in general form as

$$\lambda^3 + \epsilon_1 \lambda^2 + \epsilon_2 \lambda + \epsilon_3 + (\kappa_1 \lambda + \kappa_2) e^{-\lambda\tau} = 0, \tag{26}$$

where $\epsilon_1 = 1 + \sigma + \beta$, $\epsilon_2 = \beta\rho + \sigma + \beta\sigma$, $\epsilon_3 = \sigma\rho\beta$, $\kappa_1 = -\sigma$ and $\kappa_2 = \sigma\beta(\rho - 2)$. The equilibrium $F_n^{\pm}$ is stable if all roots of eq. (26) have negative real parts. In [25], the authors studied the distribution of the zeros of the third-degree transcendental equation (26). For completeness and convenience, the results of [25] are summarized as follows.

Clearly, $\lambda = i\omega(\omega > 0)$ is a root of eq. (26) iff ω satisfies

$$-\omega^3 i - \epsilon_1 \omega^2 + \epsilon_2 \omega i + \epsilon_3 + (\kappa_1 \omega i + \kappa_2)(\cos\omega\tau - i \sin\omega\tau) = 0.$$

Separating the real and imaginary parts, we obtain

$$\begin{cases}\epsilon_1\omega^2 - \epsilon_3 = \kappa_2 \cos\omega\tau + \kappa_1\omega\sin\omega\tau,\\ \omega^3 - \epsilon_2\omega = \kappa_1\omega\cos\omega\tau - \kappa_2\sin\omega\tau.\end{cases} \tag{27}$$

To eliminate the trigonometric functions in the above equations, we square both sides of each equation above and add the resulting equations. Thus, we have the following equation for ω:

$$\omega^6 + \varepsilon_1\omega^4 + \varepsilon_2\omega^2 + \varepsilon_3 = 0, \tag{28}$$

where $\varepsilon_1 = \epsilon_1^2 - 2\epsilon_2$, $\varepsilon_2 = \epsilon_2^2 - 2\epsilon_1\epsilon_3 - \kappa_1^2$, and $\varepsilon_3 = \epsilon_3^2 - \kappa_2^2$. Let $\mu = \omega^2$, then eq. (28) becomes

$$h(\mu) = \mu^3 + \varepsilon_1\mu^2 + \varepsilon_2\mu + \varepsilon_3 = 0. \tag{29}$$

Clearly, the function $h(\mu)$ is monotone increasing in $\mu \geq 0$ if $\Delta_1 = \varepsilon_1^2 - 3\varepsilon_2 \leq 0$. So, $h(\mu)$ has no positive real roots when $\varepsilon_3 > 0$ and $\Delta_1 \leq 0$. Furthermore, when $\varepsilon_3 \geq 0$ and $\Delta_1 > 0$, $\frac{\mathrm{d}h}{\mathrm{d}\mu} = 0$ has two real roots:

$$\mu_1^* = \frac{-\varepsilon_1 + \sqrt{\Delta_1}}{3}, \qquad \mu_2^* = \frac{-\varepsilon_1 - \sqrt{\Delta_1}}{3}.$$

Therefore, applying the results of refs. [20,25], the following lemma is obtained.

Lemma 2. *For the polynomial equation* (29)*, we have the following results:*

1) *Equation* (29) *has at least one positive root, if $\varepsilon_3 < 0$, while it does not have positive roots when $\varepsilon_3 \geq 0$ and $\Delta_1 = \varepsilon_1^2 - 3\varepsilon_2 \leq 0$.*
2) *Equation* (29) *has two positive roots, μ_1 and μ_2, if $\varepsilon_3 \geq 0, \Delta_1 = \varepsilon_1^2 - 3\varepsilon_2 > 0$, $\mu_1^* = \frac{1}{3}(-\varepsilon_1 + \sqrt{\Delta_1}) > 0$ and $h(\mu_1^*) \leq 0$.*

Without loss of generality, it is supposed that eq. (29) has three positive roots μ_k $(k = 1,2,3)$. From (27), we obtain

$$\tau_k^{(j)} = \frac{1}{\omega_k}\left[\arctan\left(\frac{(\epsilon_1\kappa_1 - \kappa_2)\,\omega_k^3 + (\epsilon_2\kappa_2 - \epsilon_3\kappa_1)\,\omega_k}{\omega_k^2\,(\epsilon_1\kappa_2 + \kappa_1\omega_k^2 - \epsilon_2\kappa_1) - \epsilon_3\kappa_2}\right) + 2\pi j\right], \quad k = 1,2,3;\ j = 0,1,\ldots. \tag{30}$$

Then $\pm i\omega_k$ is a pair of purely imaginary roots of eq. (26) with $\tau = \tau_k^{(j)}$ $(k = 1,2,3;\ j = 0,1,\ldots)$.

Define

$$\tau_0 = \tau_0^{(0)} = \min_{1\leq k\leq 3}\left\{\tau_k^{(0)}\right\}, \qquad \omega_0 = \omega_{k_0}. \tag{31}$$

Furthermore, when $\tau = 0$, eq. (26) becomes

$$\lambda^3 + \epsilon_1\lambda^2 + (\epsilon_2 + \kappa_1)\lambda + \epsilon_3 + \kappa_2 = 0. \tag{32}$$

Applying the Routh-Hurwitz criterion, all roots of this equation have negative real parts, iff

$$\epsilon_1 > 0, \epsilon_3 + \kappa_2 > 0 \quad \text{and} \quad \epsilon_1(\epsilon_2 + \kappa_1) - (\epsilon_3 + \kappa_2) > 0. \tag{33}$$

Lemma 3. [25]. *Suppose that* (33) *holds, for the third-degree transcendental equation* (26)*. Thus,*

1) *all roots of eq.* (26) *have negative real parts for all $\tau \geq 0$ if $\varepsilon_3 \geq 0$ and $\Delta_1 = \varepsilon_1^2 - 3\varepsilon_2 \leq 0$;*
2) *all roots of eq.* (26) *have negative real parts for $\tau \in [0, \tau_0)$ if one of the following holds: i) $\varepsilon_3 < 0$; ii) $\varepsilon_3 \geq 0$, $\mu_1 = \frac{1}{3}(-\varepsilon_1 + \sqrt{\Delta_1}) > 0$ and $h(\mu_1) \leq 0$.*

Additionally, we investigate the sign of

$$G = \operatorname{sign}\left\{\frac{\mathrm{d}}{\mathrm{d}\tau} Re\left(\lambda(\tau)\right)\right\}_{\tau=\tau_k^{(j)}}.$$

Lemma 4. *Suppose that $\mu_k = \omega_k^2$ and $h'(\mu_k) \neq 0$, where $h(\mu_k)$ is defined by* (29)*. Then*

$$Re\left\{\frac{\mathrm{d}\lambda}{\mathrm{d}\tau}\right\}_{\tau=\tau_k^{(j)}} \neq 0,$$

and $Re\{\frac{\mathrm{d}\lambda}{\mathrm{d}\tau}\}_{\tau=\tau_k^{(j)}}$ and $h'(\mu_k)$ have the same sign.

Proof. Differentiating the transcendental equation (26) with respect to τ, we get

$$\left(3\lambda^2+2\epsilon_1\lambda+\epsilon_2+e^{-\lambda\tau}\left(\kappa_1-\tau\left(\kappa_1\lambda+\kappa_2\right)\right)\right)\frac{\mathrm{d}\lambda}{\mathrm{d}\tau}=\lambda\left(\kappa_1\lambda+\kappa_2\right)e^{-\lambda\tau}.$$

Thus

$$\left(\frac{\mathrm{d}\lambda}{\mathrm{d}\tau}\right)^{-1}=\frac{3\lambda^2+2\epsilon_1\lambda+\epsilon_2}{\lambda(\kappa_1\lambda+\kappa_2)}e^{\lambda\tau}+\frac{\kappa_1}{\lambda(\kappa_1\lambda+\kappa_2)}-\frac{\tau}{\lambda}\,, \tag{34}$$

but

$$e^{\lambda\tau}=-\frac{\kappa_1\lambda+\kappa_2}{\lambda^3+\epsilon_1\lambda^2+\epsilon_2\lambda+\epsilon_3}\,,$$

so eq. (34) can be written as

$$\left(\frac{\mathrm{d}\lambda}{\mathrm{d}\tau}\right)^{-1}=\frac{3\lambda^2+2\epsilon_1\lambda+\epsilon_2}{-\lambda(\lambda^3+\epsilon_1\lambda^2+\epsilon_2\lambda+\epsilon_3)}+\frac{\kappa_1}{\lambda(\kappa_1\lambda+\kappa_2)}-\frac{\tau}{\lambda}\,.$$

Therefore,

$$\begin{aligned}
\operatorname{sign}\left\{\frac{\mathrm{d}}{\mathrm{d}\tau}Re\left(\lambda(\tau)\right)\right\}_{\lambda=i\omega_k} &= \operatorname{sign}\left\{Re\left(\frac{\mathrm{d}\lambda(\tau)}{\mathrm{d}\tau}\right)^{-1}\right\}_{\lambda=i\omega_k}\\
&= \operatorname{sign}\left\{Re\left(\frac{3\lambda^2+2\epsilon_1\lambda+\epsilon_2}{-\lambda(\lambda^3+\epsilon_1\lambda^2+\epsilon_2\lambda+\epsilon_3)}\right)+Re\left(\frac{\kappa_1}{\lambda(\kappa_1\lambda+\kappa_2)}\right)\right\}_{\lambda=i\omega_k}\\
&= \operatorname{sign}\left\{\frac{3\omega_k^4+2(\epsilon_1^2-2\epsilon_2)\omega_k^2+\epsilon_2^2-2\epsilon_1\epsilon_3}{\omega_k^6+(2\epsilon_1^2-\epsilon_2)\omega_k^4+(\epsilon_2^2-2\epsilon_1\epsilon_3)\omega_k^2+\epsilon_3^2}-\frac{\kappa_1^2}{\kappa_1^2\omega_k^2+\kappa_2^2}\right\}.
\end{aligned} \tag{35}$$

By using (28), we obtain

$$\omega_k^6+\left(2\epsilon_1^2-\epsilon_2\right)\omega_k^4+\left(\epsilon_2^2-2\epsilon_1\epsilon_3\right)\omega_k^2+\epsilon_3^2=\kappa_1^2\omega_k^2+\kappa_2^2.$$

Therefore,

$$\begin{aligned}
\operatorname{sign}\left\{\frac{\mathrm{d}}{\mathrm{d}\tau}Re\left(\lambda(\tau)\right)\right\}_{\lambda=i\omega_k} &= \operatorname{sign}\left\{\frac{1}{\kappa_1^2\omega_k^2+\kappa_2^2}\left(3\omega_k^4+2\left(2\epsilon_1^2-\epsilon_2\right)\omega_k^2+\epsilon_2^2-2\epsilon_1\epsilon_3-\kappa_1^2\right)\right\}\\
&= \operatorname{sign}\left\{\frac{1}{\kappa_1^2\omega_k^2+\kappa_2^2}\left(3\mu_k^2+2\varepsilon_1\mu_k+\varepsilon_2\right)\right\}\\
&= \operatorname{sign}\left\{\frac{1}{\Lambda}h'\left(\mu_k\right)\right\}\neq 0,
\end{aligned}$$

where $\Lambda=\kappa_1^2\omega_k^2+\kappa_2^2>0$. So we conclude that $Re\{\frac{\mathrm{d}\lambda}{\mathrm{d}\tau}\}_{\lambda=i\omega_k}$ and $h'(\mu_k)$ have the same sign.

As a result, the following theorem is concluded.

Theorem 2. *Let $\tau_k^{(j)}$, τ_0 and ω_0 are defined by eqs.* (30) *and* (31)*, respectively. Suppose that the condition* (33) *holds, the following results hold:*

1) *The fixed point $F_n^{\pm}$ of system* (4) *is asymptotically stable for all $\tau\geq 0$ if $\varepsilon_3\geq 0$ and $\Delta_1=\varepsilon_1^2-3\varepsilon_2\leq 0$, while it is asymptotically stable for $\tau\in[0,\tau_0)$ if either $\varepsilon_3<0$ or $\varepsilon_3\geq 0$, $\mu_1=\frac{1}{3}(-\varepsilon_1+\sqrt{\Delta_1})>0$ and $h(\mu_1)\leq 0$.*
2) *System* (4) *undergoes a Hopf bifurcation at the equilibrium $F_n^{\pm}$ when $\tau=\tau_k^{(j)}$ if one of the conditions of lemma* 3 *are satisfied, and $h'(\mu_k)\neq 0$.*

3 Hopf bifurcation of system (4)

In the previous section, we established that system (4) undergoes the Hopf bifurcation at the fixed points F_0 and $F_n^{\pm}$ when the constant delay τ passes through some certain critical values. In this section, the stability of the bifurcating periodic solutions of system (4) is discussed. To solve this problem, the center manifold theorem and the normal form method approached by Hassard *et al.* [24] are utilized. Thus, we assume that system (4) undergoes Hopf bifurcations at general steady state $F=(x_1^*,\ldots,x_n^*,y_1^*,\ldots,y_n^*,z^*)$ for $\tau=\tau_0$. Then $\pm i\omega_0$ is the corresponding purely imaginary root of the characteristic equation at equilibrium $F=(x_1^*,\ldots,x_n^*,y_1^*,\ldots,y_n^*,z^*)$.

Let $u_l = X_l - x_l^*$, $u_{l+n} = Y_l - y_l^*$, $u_{2n+1} = Z - z^*$, $(l = 1, 2, \ldots, n)$, and $\tau = \tau_0 + \eta$, where $\eta \in \mathbb{R}$. Rescaling the time delay $t \longmapsto (\frac{t}{\tau})$, then system (4) can be written as a functional differential equation in $C = C([-\tau_0, 0], \mathbb{R}^{2n+1})$ as

$$\dot{\boldsymbol{u}}(t) = \boldsymbol{B}_\eta\left(\boldsymbol{u}(t)\right) + \boldsymbol{f}\left(\eta, \boldsymbol{u}(t)\right), \tag{36}$$

where $\boldsymbol{u}(t) = (u_1(t), u_2(t), \ldots, u_n(t), u_{n+1}(t), \ldots, u_{2n}(t), u_{2n+1}(t))^T \in \mathbb{R}^{2n+1}$, and $\boldsymbol{B}_\eta : C \to \mathbb{R}, \boldsymbol{f} : \mathbb{R} \times C \to \mathbb{R}$ are given, respectively, by

$$\begin{aligned}\boldsymbol{B}_\eta(\boldsymbol{\phi}) = {} & (\tau_0 + \eta)\begin{pmatrix} -\sigma\boldsymbol{I}_n & 0\boldsymbol{I}_n & \boldsymbol{0} \\ (\rho - z^*)\boldsymbol{I}_n & -\boldsymbol{I}_n & -\boldsymbol{x}^* \\ \boldsymbol{y}^{*T} & \boldsymbol{x}^{*T} & -\beta \end{pmatrix}\begin{pmatrix} \boldsymbol{\phi}_n(0) \\ \boldsymbol{\phi}_{2n}(0) \\ \phi_{2n+1}(0) \end{pmatrix} \\ & + (\tau_0 + \eta)\begin{pmatrix} 0\boldsymbol{I}_n & \sigma\boldsymbol{I}_n & \boldsymbol{0} \\ 0\boldsymbol{I}_n & 0\boldsymbol{I}_n & \boldsymbol{0} \\ \boldsymbol{0}^T & \boldsymbol{0}^T & 0 \end{pmatrix}\begin{pmatrix} \boldsymbol{\phi}_n(-\tau_0) \\ \boldsymbol{\phi}_{2n}(-\tau_0) \\ \phi_{2n+1}(-\tau_0) \end{pmatrix}\end{aligned} \tag{37}$$

and

$$\boldsymbol{f}(\eta, \boldsymbol{\phi}) = (\tau_0 + \eta)\begin{pmatrix} \boldsymbol{0} \\ -\phi_{2n+1}(0)\boldsymbol{\phi}_n(0) \\ \left(\boldsymbol{\phi}_n(0)\right)^T \boldsymbol{\phi}_{2n}(0) \end{pmatrix}, \tag{38}$$

where $\boldsymbol{\phi} = (\boldsymbol{\phi}_n, \boldsymbol{\phi}_{2n}, \phi_{2n+1})^T \in C^1([-\tau_0, 0], \mathbb{R}^{2n+1}), \boldsymbol{\phi}_n = (\phi_1, \phi_2, \ldots, \phi_n)^T, \boldsymbol{\phi}_{2n} = (\phi_{n+1}, \phi_{n+2}, \ldots, \phi_{2n})^T$.

Using the Riesz representation theorem, $(2n + 1) \times (2n + 1)$ exists, such that

$$\boldsymbol{B}_\eta\boldsymbol{\phi} = \int_{-\tau_0}^{0} \mathrm{d}\boldsymbol{\xi}(\theta, \eta)\boldsymbol{\phi}(\theta) \quad \text{for } \boldsymbol{\phi} \in C^1\left([-\tau_0, 0], \mathbb{R}^{2n+1}\right). \tag{39}$$

According to the algorithm of [24], $\boldsymbol{\xi}(\theta, \eta)$ can be expressed as

$$\boldsymbol{\xi}(\theta, \eta) = (\tau_0 + \eta)\begin{pmatrix} -\sigma\boldsymbol{I}_n & 0\boldsymbol{I}_n & \boldsymbol{0} \\ (\rho - z^*)\boldsymbol{I}_n & -\boldsymbol{I}_n & -\boldsymbol{x}^* \\ \boldsymbol{y}^{*T} & \boldsymbol{x}^{*T} & -\beta \end{pmatrix}\delta(\theta) - (\tau_0 + \eta)\begin{pmatrix} 0\boldsymbol{I}_n & \sigma\boldsymbol{I}_n & \boldsymbol{0} \\ 0\boldsymbol{I}_n & 0\boldsymbol{I}_n & \boldsymbol{0} \\ \boldsymbol{0}^T & \boldsymbol{0}^T & 0 \end{pmatrix}\delta(\theta + \tau_0), \tag{40}$$

where $\delta(\theta)$ is the Dirac delta function. For $\boldsymbol{\phi} \in C^1([-\tau_0, 0], \mathbb{R}^{2n+1})$, $\boldsymbol{E}(\eta)\boldsymbol{\phi}$ and $\boldsymbol{Q}(\eta)\boldsymbol{\phi}$ are expressed as [24]

$$\boldsymbol{E}(\eta)\boldsymbol{\phi} = \begin{cases} \dfrac{\mathrm{d}\boldsymbol{\phi}}{\mathrm{d}\theta}, & \theta \in [-\tau_0, 0), \\ \displaystyle\int_{-\tau_0}^{0} \mathrm{d}\boldsymbol{\xi}(\theta, s)\boldsymbol{\phi}(s) = \boldsymbol{B}_\eta\boldsymbol{\phi}, & \theta = 0, \end{cases} \tag{41}$$

and

$$\boldsymbol{Q}(\eta)\boldsymbol{\phi} = \begin{cases} \boldsymbol{0}, & \theta \in [-\tau_0, 0), \\ \boldsymbol{f}\left(\eta, \boldsymbol{\phi}\right), & \theta = 0. \end{cases} \tag{42}$$

Since $\mathrm{d}\boldsymbol{u}_t/\mathrm{dt} = \mathrm{d}\boldsymbol{u}_t/\mathrm{d}\theta$, system (36) can be rewritten as

$$\dot{\boldsymbol{u}}_t = \boldsymbol{E}(\eta)\boldsymbol{u}_t + \boldsymbol{Q}(\eta)\boldsymbol{u}_t, \tag{43}$$

where $\boldsymbol{u}_t(\theta) = \boldsymbol{u}(t + \theta)$.

For $\boldsymbol{\psi} \in C^1([0, \tau_0], \mathbb{R}^{2n+1})$, the adjoint operator $\boldsymbol{E}^*$ of $\boldsymbol{E}$ is defined as

$$\boldsymbol{E}^*\boldsymbol{\psi}(s) = \begin{cases} -\dfrac{\mathrm{d}\boldsymbol{\psi}(s)}{\mathrm{d}s}, & s \in (0, \tau_0], \\ \displaystyle\int_{-\tau_0}^{0} \mathrm{d}\boldsymbol{\xi}^T(t, 0)\boldsymbol{\psi}(-t), & s = 0. \end{cases} \tag{44}$$

Note that the domains of $\boldsymbol{E}(0)$ and $\boldsymbol{E}^*$ are $C^1([-\tau_0,0],\mathbb{R}^{2n+1})$ and $C^1([0,\tau_0],\mathbb{R}^{2n+1})$, respectively. For $\boldsymbol{\phi}\in C^1([-\tau_0,0],\mathbb{R}^{2n+1})$ and $\boldsymbol{\psi}\in C^1([0,\tau_0],\mathbb{R}^{2n+1})$, the bilinear form is defined as follows:

$$\langle\boldsymbol{\psi}(s),\boldsymbol{\phi}(\theta)\rangle=\bar{\boldsymbol{\psi}}(0)\boldsymbol{\phi}(0)-\int_{\theta=-\tau_0}^{0}\int_{\zeta=0}^{\theta}\bar{\boldsymbol{\psi}}(\zeta-\theta)\,\mathrm{d}\boldsymbol{\xi}(\theta)\boldsymbol{\phi}(\zeta)\mathrm{d}\zeta, \tag{45}$$

where $\boldsymbol{\xi}(\theta)=\boldsymbol{\xi}(\theta,0)$. Then $\boldsymbol{E}(0)$ and $\boldsymbol{E}^*$ are adjoint operators. From the results of sect. 3, we got that $\pm i\omega_0\tau_0$ are eigenvalues of $\boldsymbol{E}(0)$, and they are also eigenvalues of $\boldsymbol{E}^*$.

For $\theta\in[-\tau_0,0]$, it is assumed that the eigenvector of $\boldsymbol{E}(0)$, which corresponds to the eigenvalue $i\omega_0\tau_0$, is $\boldsymbol{\nu}(\theta)=(1,\alpha_1,\alpha_2,\ldots,\alpha_n,\gamma_1,\gamma_2,\ldots,\gamma_n)^Te^{i\omega_0\tau_0\theta}$, then $\boldsymbol{E}(0)\boldsymbol{\nu}(\theta)=i\omega_0\tau_0\boldsymbol{\nu}(\theta)$. According to the definition of $\boldsymbol{E}(0)$ and $\boldsymbol{\xi}(\theta,\eta)$,

$$\tau_0\begin{pmatrix}(i\omega_0+\sigma)\boldsymbol{I}_n & -\sigma e^{-i\omega_0\tau_0}\boldsymbol{I}_n & \boldsymbol{0}\\ (z^*-\rho)\boldsymbol{I}_n & (i\omega_0+1)\boldsymbol{I}_n & \boldsymbol{x}^*\\ -\boldsymbol{y}^{*T} & -\boldsymbol{x}^{*T} & i\omega_0+\beta\end{pmatrix}\boldsymbol{\nu}(0)=\begin{pmatrix}\boldsymbol{0}\\ \boldsymbol{0}\\ 0\end{pmatrix}. \tag{46}$$

Thus, it is easy to obtain the following:

$$\begin{aligned}
\alpha_k&=\frac{\sigma\Omega_0}{\Omega_1e^{iw_0\tau_0}+\Omega_2}x^*_{k+1},\quad k=1,2,\ldots,n-1,\\
\alpha_n&=\frac{\Omega_3+\Omega_4}{-(\Omega_1+\Omega_2)},\\
\gamma_k&=\frac{(i\omega_0+\sigma)\Omega_0}{\Omega_1+\Omega_2e^{-iw_0\tau_0}}x^*_{k+1},\quad k=1,2,\ldots,n-1,\\
\gamma_n&=\frac{\Omega_0(e^{iw_0\tau_0}(1+i\omega_0)(i\omega_0+\sigma)+\sigma(z^*-\rho))}{\Omega_1e^{iw_0\tau_0}-\Omega_2},\\
\Omega_0&=y^*_1(1+i\omega_0)+x^*_1(\rho-z^*),\\
\Omega_1&=(1+i\omega_0)(i\omega_0+\sigma)\left(\sum_{l=1}^n(x^*_l)^2-\omega_0+\beta+i\omega_0(1+\beta)\right),\\
\Omega_2&=\sigma\left((-1-i\omega_0)\sum_{l=2}^n x^*_ly^*_l+(z^*-\rho)\left(\omega_0-(x^*_1)^2-\beta-i\omega_0(1+\beta)\right)\right),\\
\Omega_3&=(\omega_0-i\sigma)e^{iw_0\tau_0}\left((\omega_0-i)x^*_1y^*_1+(z^*-\rho)\left(\omega_0(1+\beta+i\omega_0)-i\left(\beta+\sum_{l=2}^n(x^*_l)^2\right)\right)\right),\\
\Omega_4&=-\sigma(z^*-\rho)\left(\sum_{l=1}^n x^*_ly^*_l+(\beta+i\omega_0)(z^*-\rho)\right).
\end{aligned} \tag{47}$$

Similarly, let $\boldsymbol{\nu}^*(\theta)=D(1,\alpha^*_1,\alpha^*_2,\ldots,\alpha^*_n,\gamma^*_1,\gamma^*_2,\ldots,\gamma^*_n)e^{i\omega_0\tau_0s}$ $(s\in[-1,0])$ be the eigenvector of $\boldsymbol{E}^*$ corresponding to the eigenvalue $-i\omega_0\tau_0$, and similarly we get

$$\begin{aligned}
\alpha^*_k&=\frac{\sigma x^*_1e^{iw_0\tau_0}((i\omega_0-1)y^*_{k+1}+(z^*-\rho)x^*_{k+1})}{-(\bar{\Omega}_1+\bar{\Omega}_2e^{iw_0\tau_0})},\quad k=1,2,\ldots,n-1,\\
\alpha^*_n&=\frac{\sigma^{iw_0\tau_0}(\Omega_5+\Omega_6)}{\bar{\Omega}_1+\bar{\Omega}_2e^{iw_0\tau_0}},\\
\gamma^*_k&=\frac{\sigma x^*_1e^{iw_0\tau_0}(x^*_{k+1}(\sigma-i\omega_0)+\sigma y^*_{k+1}e^{iw_0\tau_0})}{\bar{\Omega}_1+\bar{\Omega}_2e^{iw_0\tau_0}},\quad k=1,2,\ldots,n-1,\\
\gamma^*_n&=\frac{\sigma x^*_1e^{iw_0\tau_0}(\omega_0+\sigma((\rho-z^*)e^{iw_0\tau_0}-1)+i\omega_0(1+\sigma))}{-(\bar{\Omega}_1+\bar{\Omega}_2e^{iw_0\tau_0})},\\
\Omega_5&=(\omega_0+i\sigma)\left(\omega_0(1+\beta-i\omega_0)+i\left(\beta+\sum_{l=2}^n(x^*_l)^2\right)\right),\\
\Omega_6&=-\sigma e^{iw_0\tau_0}\left(\sum_{l=2}^n x^*_ly^*_l+(\beta-i\omega_0)(z^*-\rho)\right).
\end{aligned} \tag{48}$$

Using (45), we obtain:

$$
\begin{aligned}
\langle \boldsymbol{\nu}^*(s), \boldsymbol{\nu}(\theta)\rangle &= \bar{\boldsymbol{\nu}}^*(0)\boldsymbol{\nu}(0) - \int_{-1}^{0}\int_{\zeta=0}^{\theta} \bar{\boldsymbol{\nu}}^*(\zeta-\theta)\,\mathrm{d}\boldsymbol{\xi}(\theta)\boldsymbol{\nu}(\zeta)\mathrm{d}\zeta \\
&= \bar{D}\left(1, \bar{\alpha}_1^*, \ldots, \bar{\alpha}_n^*, \bar{\gamma}_1^*, \ldots, \bar{\gamma}_n^*\right)\left(1, \alpha_1, \ldots, \alpha_n, \gamma_1, \ldots, \gamma_n\right)^T \\
&\quad - \int_{-1}^{0}\int_{\zeta=0}^{\theta} \bar{D}\left(1, \bar{\alpha}_1^*, \ldots, \bar{\gamma}_n^*\right) e^{-i\omega_0\tau_0(\zeta-\theta)}\mathrm{d}\boldsymbol{\xi}(\theta)\left(1, \alpha_1, \ldots, \gamma_n\right)^T e^{i\omega_0\tau_0\zeta}\mathrm{d}\zeta \\
&= \bar{D}\left(1 + \sum_{l=1}^{n}\left(\bar{\alpha}_l^*\alpha_l + \bar{\gamma}_l^*\gamma_l\right) - \int_{-1}^{0}\left(1, \bar{\alpha}_1^*, \ldots, \bar{\gamma}_n^*\right)\theta e^{i\omega_0\tau_0\theta}\mathrm{d}\boldsymbol{\xi}(\theta)\left(1, \alpha_1, \ldots, \gamma_n\right)^T\right) \\
&= \bar{D}\left(1 + \sum_{l=1}^{n}\left(\bar{\alpha}_l^*\alpha_l + \bar{\gamma}_l^*\gamma_l\right) + \sigma\tau_0 e^{-iw_0\tau_0}\left(\alpha_n + \sum_{l=1}^{n-1}\bar{\alpha}_l^*\gamma_l\right)\right).
\end{aligned}
$$

Then we choose

$$
D = \left(1 + \sum_{l=1}^{n}\left(\alpha_l^*\bar{\alpha}_l + \gamma_l^*\bar{\gamma}_l\right) + \sigma\tau_0 e^{iw_0\tau_0}\left(\bar{\alpha}_n + \sum_{l=1}^{n-1}\alpha_l^*\bar{\gamma}_l\right)\right)^{-1}, \tag{49}
$$

to satisfy $\langle \boldsymbol{\nu}^*(s), \boldsymbol{\nu}(\theta)\rangle = 1$ and $\langle \boldsymbol{\nu}^*(s), \bar{\boldsymbol{\nu}}(\theta)\rangle = 0$.

Following a computation process similar to that of [25], the following quantities can be obtained:

$$
\begin{aligned}
g_{20} &= 2\tau_0\bar{D}\left(\bar{\gamma}_n^*\left(\alpha_n + \sum_{l=1}^{n-1}\alpha_l\gamma_l\right) - \gamma_n\left(\bar{\alpha}_n^* + \sum_{l=1}^{n-1}\alpha_l\bar{\gamma}_l^*\right)\right), \\
g_{11} &= \tau_0\bar{D}\left(\bar{\gamma}_n^*\left(2Re\{\alpha_n\} + \sum_{l=1}^{n-1}\left(\bar{\alpha}_l\gamma_l + \alpha_l\bar{\gamma}_l\right)\right) - \gamma_n\left(\bar{\alpha}_n^* + \sum_{l=1}^{n-1}\bar{\alpha}_l\bar{\gamma}_l^*\right) - \bar{\gamma}_n\left(\bar{\alpha}_n^* + \sum_{l=1}^{n-1}\alpha_l\bar{\gamma}_l^*\right)\right), \\
g_{02} &= 2\tau_0\bar{D}\left(\bar{\gamma}_n^*\left(\bar{\alpha}_n + \sum_{l=1}^{n-1}\bar{\alpha}_l\bar{\gamma}_l\right) - \gamma_n\left(\bar{\alpha}_n^* + \sum_{l=1}^{n-1}\bar{\alpha}_l\bar{\gamma}_l^*\right)\right), \\
g_{21} &= \tau_0\bar{D}\Bigg(- \bar{\alpha}_n^*\left(2\varGamma_{11}^{(2n+1)}(0) + 2\gamma_n\varGamma_{11}^{(1)}(0) + \varGamma_{20}^{(2n+1)}(0) + \bar{\gamma}_n\varGamma_{20}^{(1)}(0)\right) \\
&\quad - \sum_{l=1}^{n-1}\bar{\gamma}_l^*\left(2\alpha_l\varGamma_{11}^{(2n+1)}(0) + 2\gamma_n\varGamma_{11}^{(l+1)}(0) + \bar{\alpha}_l\varGamma_{20}^{(2n+1)}(0) + \bar{\gamma}_n\varGamma_{20}^{(l+1)}(0)\right) \\
&\quad + \bar{\gamma}_n^*\Bigg(\varGamma_{11}^{(n+1)}(0) + 2\alpha_n\varGamma_{11}^{(1)}(0) + 2\sum_{l=1}^{n-1}\left(\alpha_l\varGamma_{11}^{(n+l+1)}(0) + \gamma_l\varGamma_{11}^{(l+1)}(0)\right) \\
&\quad + \varGamma_{20}^{(n+1)}(0) + \bar{\alpha}_n\varGamma_{20}^{(1)}(0) + \sum_{l=1}^{n-1}\left(\bar{\alpha}_l\varGamma_{20}^{(n+l+1)}(0) + \bar{\gamma}_l\varGamma_{20}^{(l+1)}(0)\right)\Bigg)\Bigg),
\end{aligned} \tag{50}
$$

where

$$
\begin{aligned}
\boldsymbol{\varGamma}_{20}(\theta) &= \frac{ig_{20}}{w_0\tau_0}\boldsymbol{\nu}(0)e^{iw_0\tau_0\theta} + \frac{i\bar{g}_{02}}{3w_0\tau_0}\bar{\boldsymbol{\nu}}(0)e^{-iw_0\tau_0\theta} + \boldsymbol{\varDelta}e^{2iw_0\tau_0\theta}, \\
\boldsymbol{\varGamma}_{11}(\theta) &= -\frac{ig_{11}}{w_0\tau_0}\boldsymbol{\nu}(0)e^{iw_0\tau_0\theta} + \frac{i\bar{g}_{11}}{w_0\tau_0}\bar{\boldsymbol{\nu}}(0)e^{-iw_0\tau_0\theta} + \boldsymbol{\varLambda},
\end{aligned} \tag{51}
$$

where $\boldsymbol{\varGamma}_{20} = (\varGamma_{20}^{(1)}, \varGamma_{20}^{(2)}, \ldots, \varGamma_{20}^{(2n+1)})^T$, $\boldsymbol{\varGamma}_{11} = (\varGamma_{11}^{(1)}, \varGamma_{11}^{(2)}, \ldots, \varGamma_{11}^{(2n+1)})^T$.

Also, $\boldsymbol{\Delta} = (\Delta^{(1)}, \Delta^{(2)}, \dots, \Delta^{(2n+1)})^T \in \mathbb{C}^{2n+1}$ and $\boldsymbol{\Lambda} = (\Lambda^{(1)}, \Lambda^{(2)}, \dots, \Lambda^{(2n+1)})^T \in \mathbb{C}^{2n+1}$ are constant vectors, which can be computed through the relations

$$\begin{pmatrix} (2iw_0+\sigma)\boldsymbol{I}_n & -\sigma e^{2iw_0\tau_0}\boldsymbol{I}_n & \boldsymbol{0} \\ -(\rho-z^*)\boldsymbol{I}_n & (2iw_0+1)\boldsymbol{I}_n & \boldsymbol{x}^* \\ -\boldsymbol{y}^{*T} & -\boldsymbol{x}^{*T} & 2iw_0+\beta \end{pmatrix} \cdot \boldsymbol{\Delta} = \begin{pmatrix} \boldsymbol{0} \\ -\gamma_5\boldsymbol{\alpha} \\ \alpha_n + \sum_{l=1}^{n-1} \alpha_l\gamma_l \end{pmatrix},$$

$$\begin{pmatrix} \sigma\boldsymbol{I}_n & -\sigma\boldsymbol{I}_n & \boldsymbol{0} \\ -(\rho-z^*)\boldsymbol{I}_n & \boldsymbol{I}_n & \boldsymbol{x}^* \\ -\boldsymbol{y}^{*T} & -\boldsymbol{x}^{*T} & \beta \end{pmatrix} \cdot \boldsymbol{\Lambda} = \begin{pmatrix} \boldsymbol{0} \\ -\left(\gamma_5\bar{\boldsymbol{\alpha}} + \bar{\gamma}_5\boldsymbol{\alpha}\right) \\ 2Re\{\alpha_n\} + \sum_{l=1}^{n-1} \left(\bar{\alpha}_l\gamma_l + \alpha_l\bar{\gamma}_l\right) \end{pmatrix}, \tag{52}$$

where $\boldsymbol{\alpha} = (1, \alpha_1, \alpha_2, \dots, \alpha_n)^T$.

Using eq. (50) we can compute the following values [25]:

$$\begin{aligned} c_1(0) &= \frac{i}{2\omega_0}\left(g_{11}g_{20} - 2|g_{11}|^2 - \frac{|g_{02}|^2}{3}\right) + \frac{g_{21}}{2}, \\ \eta_2 &= -\frac{Re\{c_1(0)\}}{Re\{\acute{\lambda}(0)\}}, \\ \beta_2 &= 2Re\{c_1(0)\}, \\ T_2 &= -\frac{Im\{c_1(0)\} + \eta_2 Im\{\acute{\lambda}(0)\}}{\omega_0}, \end{aligned} \tag{53}$$

where η_2 determines the directions of the Hopf bifurcation, by means the Hopf bifurcation is supercritical if $\eta_2 > 0$ and if $\eta_2 < 0$ then the Hopf bifurcation is subcritical and the bifurcating periodic solutions exists for $\tau = \tau_0$. β_2 defines the stability of the bifurcating periodic solutions: the bifurcating periodic solutions are stable (unstable) if $\beta_2 < 0$ ($\beta_2 > 0$); and T_2 determines the period of the bifurcating periodic solutions: the period increases (decreases) if $T_2 > 0$ ($T_2 < 0$).

4 Numerical simulation

This section checks numerically the validity of the analytical results of sects. 2 and 3. The stability of the trivial fixed point F_0 is investigated. Let $\sigma = 15$, $\beta = 8/3$, $n = 5$ and vary ρ. If $0 < \rho < 1$, the conditions (12) and (16) are satisfied. So from theorem 1, then the trivial fixed point F_0 is asymptotically stable for $\tau \geq 0$, as shown in fig. 1, for the case $\rho = 0.5$, $\tau = 3$. Additionally, if we choose $\rho < -1$, the conditions (12) and (17) hold, *i.e.*, system (4) is asymptotically stable for $\tau \in [0, \tau_0)$. Figure 2 shows the stability critical curve using (18) with (10) and (19) in $\rho - \tau$ parameter space, where, τ_0 is represented by the red line. It is concluded that the stable island lies between the $\tau = 0$ curve and the τ_0 curve. The shaded region in fig. 2 represents the stable zone, and the τ_0 curve represents the Hopf bifurcation curve. If $\rho = -2$, for example, and from (18) and (10) we obtain $\omega_+ = 1.717$ and $\tau_0 = 1.1556$. By choosing $\tau = 1.1 < \tau_0$, F_0 is asymptotically stable as shown in fig. 3. By theorem 1, a Hopf bifurcation occurs when $\tau_0 = 1.1556$, the origin loses its stability and a periodic solution bifurcates from the origin exists for $\tau = 1.19 > \tau_0$, as displayed in figs. 4 and 5. From eqs. (53) in sect. 3, it follows that:

$$\begin{aligned} c_1(0) &= -0.0477954 + 0.0155392i, \\ Re\{\acute{\lambda}(0)\} &= 0.320481, \\ Im\{\acute{\lambda}(0)\} &= -1.06822, \\ \eta_2 &= 0.149137 > 0, \\ \beta_2 &= -0.0955909 < 0, \\ T_2 &= 0.0837316 > 0. \end{aligned} \tag{54}$$

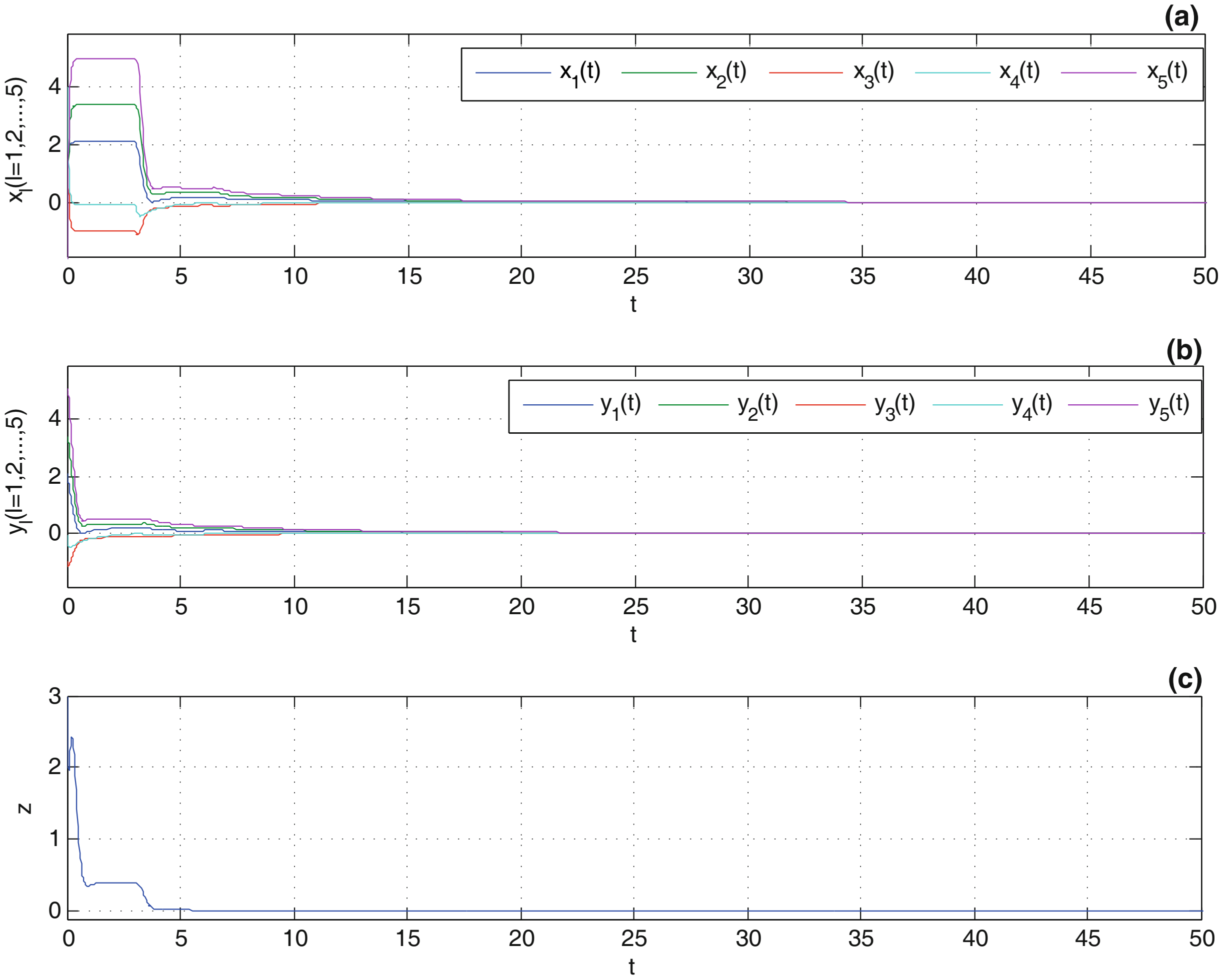

Fig. 1. Solution curve of the system (4) for $\sigma = 15$, $\beta = 8/3$, $n = 5$, $\rho = 0.5$, and $\tau = 3$. By means, the conditions (12) and (16) satisfied, the trivial fixed point F_0 is asymptotically stable for any $\tau \geq 0$. (a) A state space in the (t, x_l) plane, $l = 1, 2, \ldots, 5$. (b) A state space in the (t, y_l)-plane. (c) A state space in the (t, z)-plane.

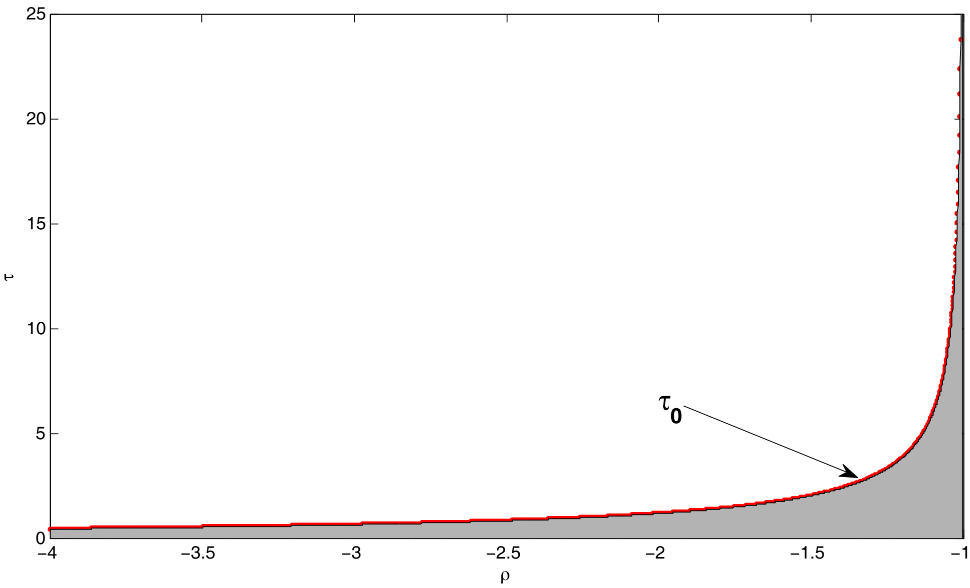

Fig. 2. Stability zone in the ρ-τ parameter space with parameters $\sigma = 15$, $\beta = 8/3$, $n = 5$. Shaded region indicates the zone of stable trivial fixed point F_0.

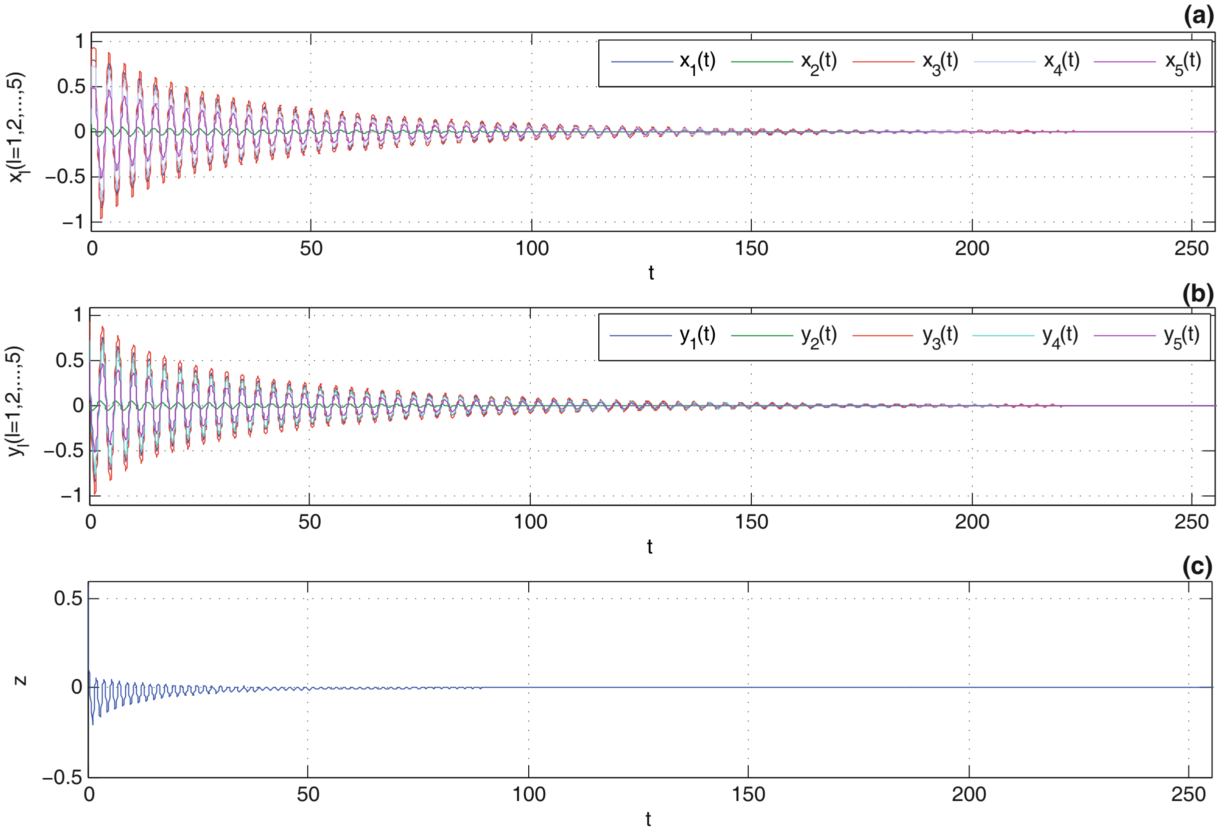

Fig. 3. Solution curve of the system (4) for $\sigma = 15$, $\beta = 8/3$, $n = 5$, $\rho = -2$, and $\tau = 1.1 < \tau_0$. The origin of this system is asymptotically stable. (a) A state space in the (t, x_l)-plane, $l = 1, 2, \dots, 5$. (b) A state space in the (t, y_l)-plane. (c) A state space in the (t, z)-plane.

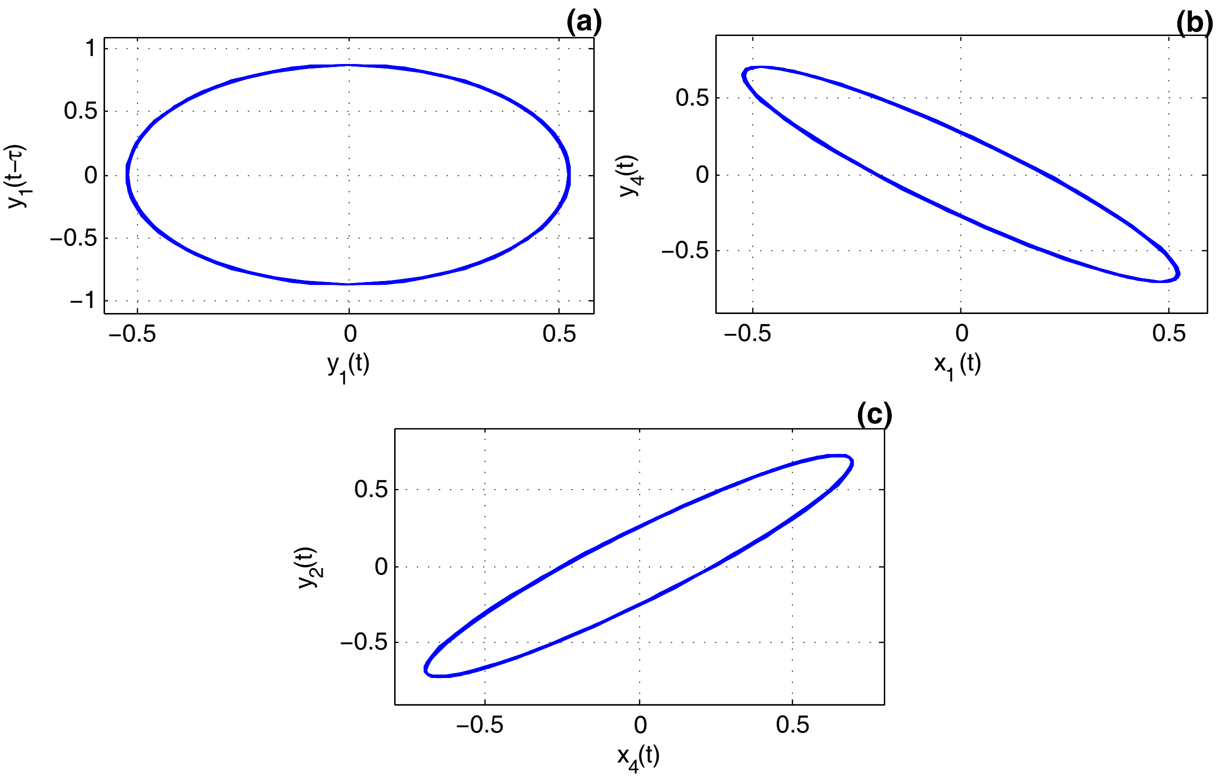

Fig. 4. Bifurcating periodic solution for the system (4) for $\sigma = 15$, $\beta = 10$, $n = 5$, $\rho = -2$, and $\tau = 1.19 > \tau_0$. (a) $(y_1(t), y_1(t-\tau))$-plane. (b) $(x_1(t), y_4(t))$-plane. (c) $(x_4(t), y_2(t))$-plane.

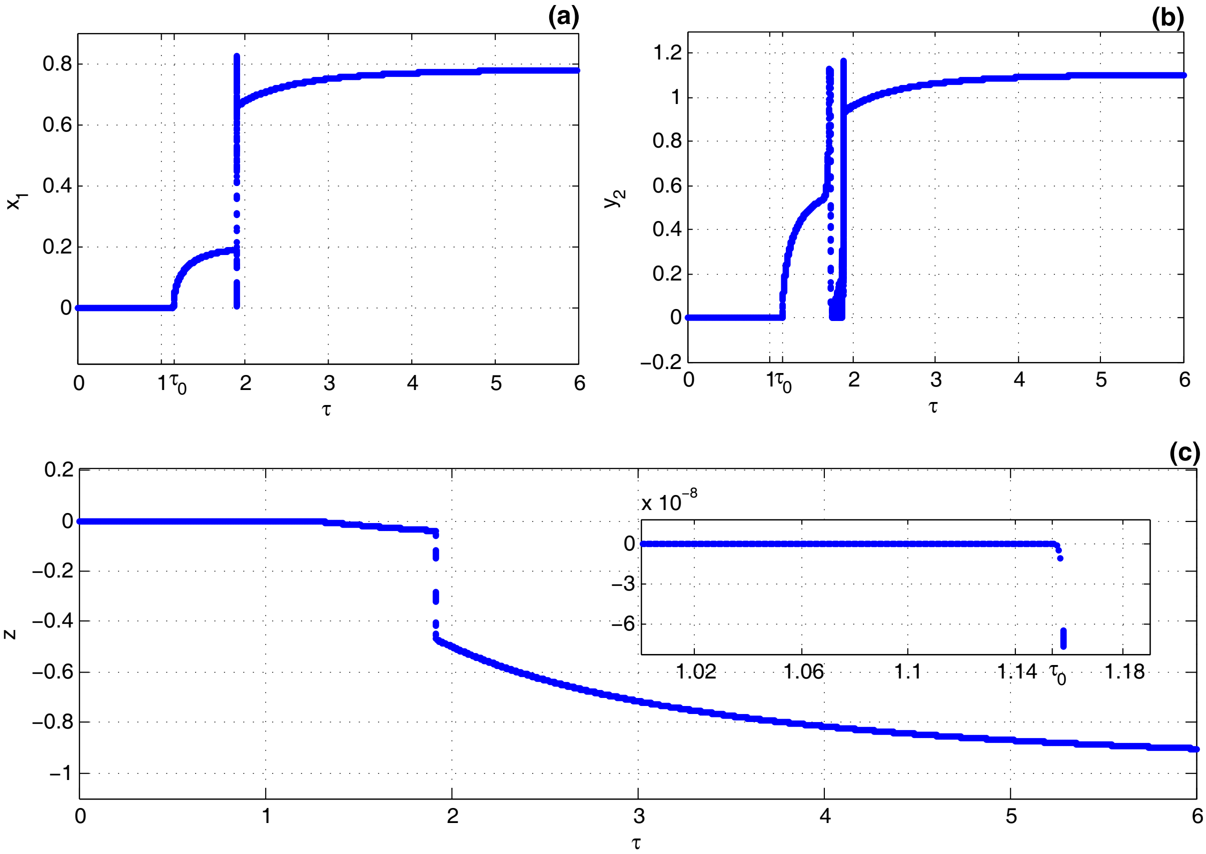

Fig. 5. Bifurcation diagrams of time delay system (4) for the parameters values $\sigma = 15$, $\beta = 8/3$, $n = 5$, $\rho = -2$. (a) $x_1(t)$ *versus* τ. (b) $y_2(t)$ *versus* τ. (c) $z(t)$ *versus* τ.

Since $\eta_2 > 0$ and $\beta_2 < 0$, the Hopf bifurcation is supercritical and the direction of the bifurcation is $\tau > \tau_0$. These bifurcating periodic solutions from F_0 at τ_0 are stable, as shown in figs. 4 and 5. Finally, since $T_2 > 0$ the period of the limit cycle increases with increasing τ. We can summarize these observations through the bifurcation diagram in fig. 5. Figure 5 shows the bifurcation diagram of x_1, y_2, z *versus* τ with $\rho = -2$. Clearly, when $\tau < \tau_0 = 1.1556$ the solution is asymptotically stable, when $\tau = \tau_0$ the Hopf bifurcation occurs. Finally when $\tau > \tau_0$ the periodic solution appears.

Concerning the stability of the nontrivial fixed point F_n^+, we choose $\sigma = 6$, $\beta = 1$, $\rho = 8$, $n = 5$, and we get that eq. (28) has two positive roots $\omega_1 = 1.78089$ and $\omega_2 = 2.97127$. Therefore, we obtain

$$\tau_1^{(j)} = 1.08315 + 3.52811j, \quad \tau_2^{(j)} = 0.172541 + 2.11465j, \quad j = 0, 1, \ldots.$$

From formula (53), it follows that $c_1(0) = 0.0120439 - 0.199998i$, $\eta_2 = -0.01831 < 0$, $\beta_2 = 0.0240878 > 0$, $T_2 = 0.0553719 > 0$. Thus, the equilibria F_n^+ is stable for $\tau < \tau_2^{(0)}$ as illustrated by the numerical simulation, see fig. 6. When τ passes through the critical value $\tau_2^{(0)}$, F_n^+ loses its stability and a Hopf bifurcation occurs as shown in fig. 7. Since $\eta_2 < 0$, $\beta_2 > 0$, the Hopf bifurcation is subcritical and the direction of the Hopf bifurcation is $\tau > \tau_2^{(0)}$. These bifurcating periodic solutions from F_n^+ are unstable as depicted in fig. 7, where chaos appears. Moreover, it is interesting to simulate the bifurcation diagram in fig. 8 for system (4). Figure 8 illustrates that when τ increases the nontrivial equilibrium F_n^+ becomes stable for $[0, \tau_2^{(0)})$ and a Hopf bifurcation occurs when τ crosses a critical value $\tau_2^{(0)}$. After that chaotic solution appears which confirms our results of figs. 6 and 7.

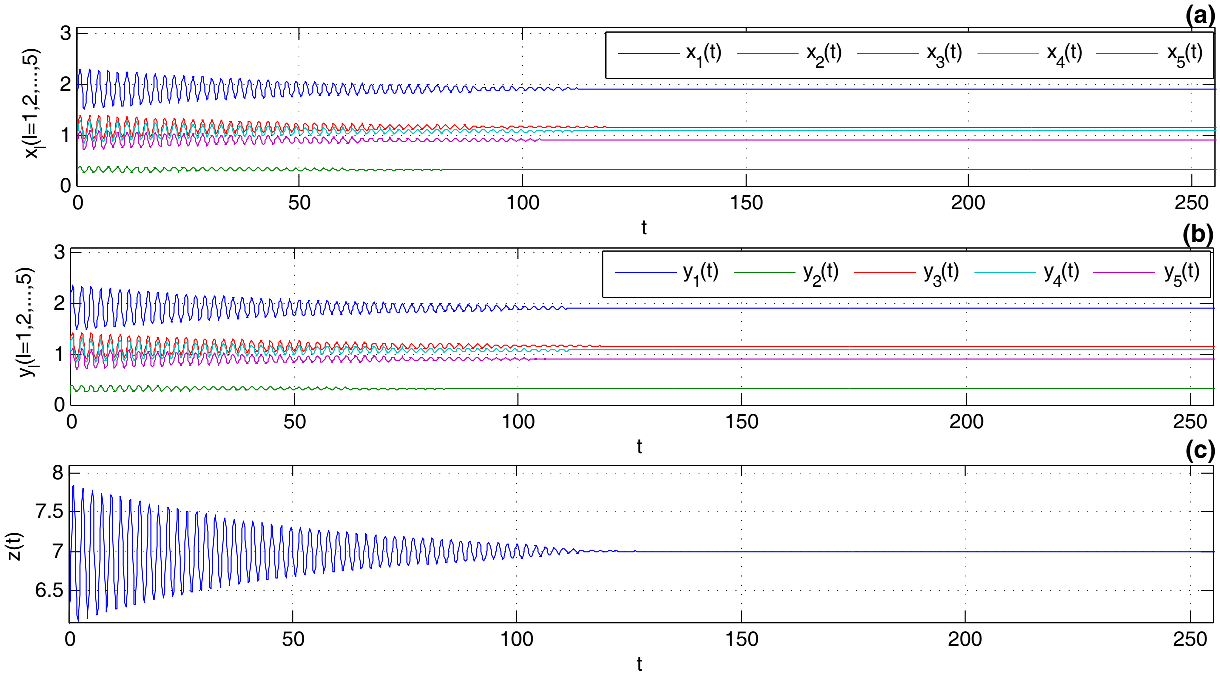

Fig. 6. Solution curve of the system (4) for $\sigma = 6$, $\beta = 1$, $n = 5$, $\rho = 8$ and $\tau = 0.16 < \tau_2^{(0)}$. The nontrivial fixed point F_n^+ is stable. (a) A state space in the (t, x_l)-plane, $l = 1, 2, \ldots, 5$. (b) A state space in the (t, y_l)-plane. (c) A state space in the (t, z)-plane.

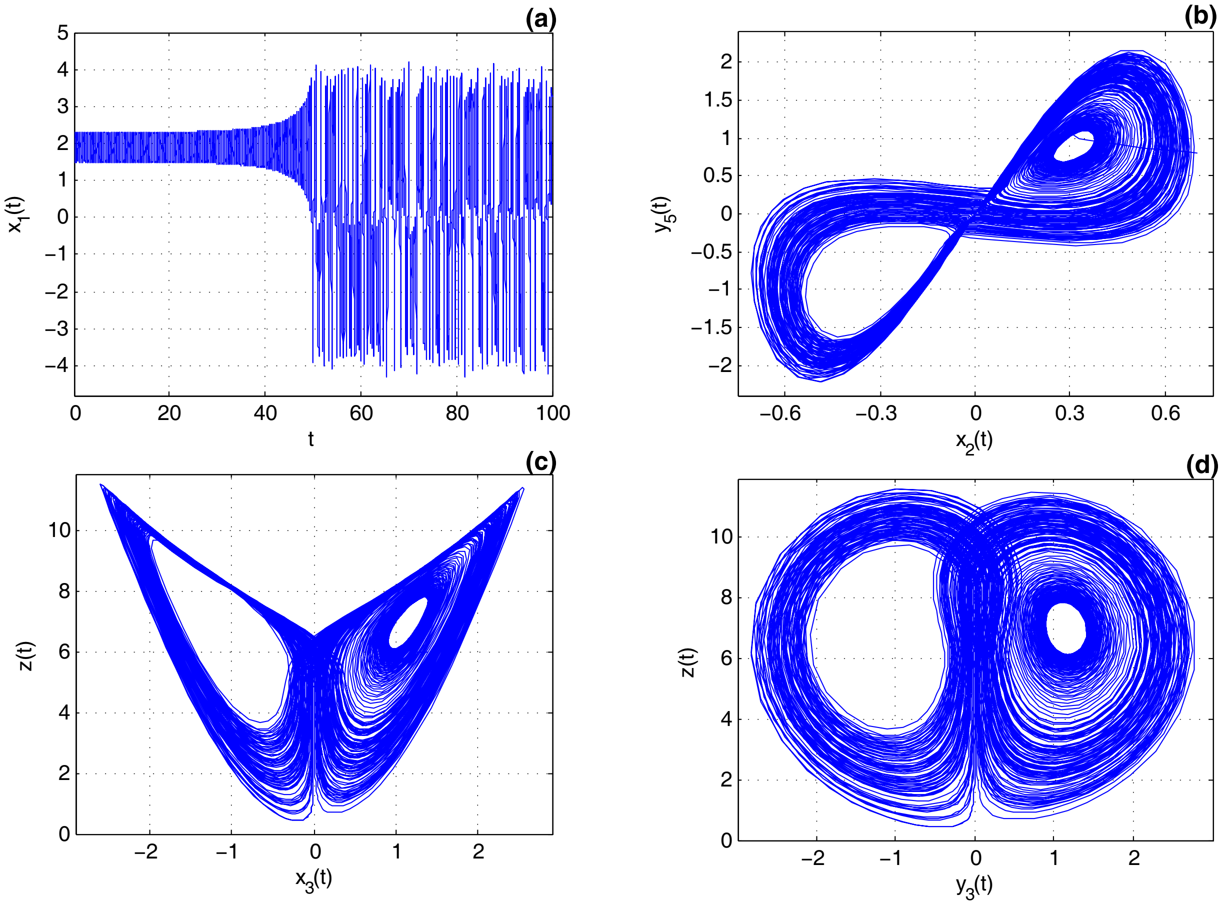

Fig. 7. Chaos solution when $\tau = 0.18 > \tau_2^{(0)}$, $\sigma = 6$, $\beta = 1$, $n = 5$, $\rho = 8$. The nontrivial fixed point F_n^+ is unstable. (a) A state space in the (t, x_1)-plane. (b) $(x_2(t), y_5(t))$-plane. (c) $(x_3(t), z(t))$-plane. (c) $(y_3(t), z(t))$-plane.

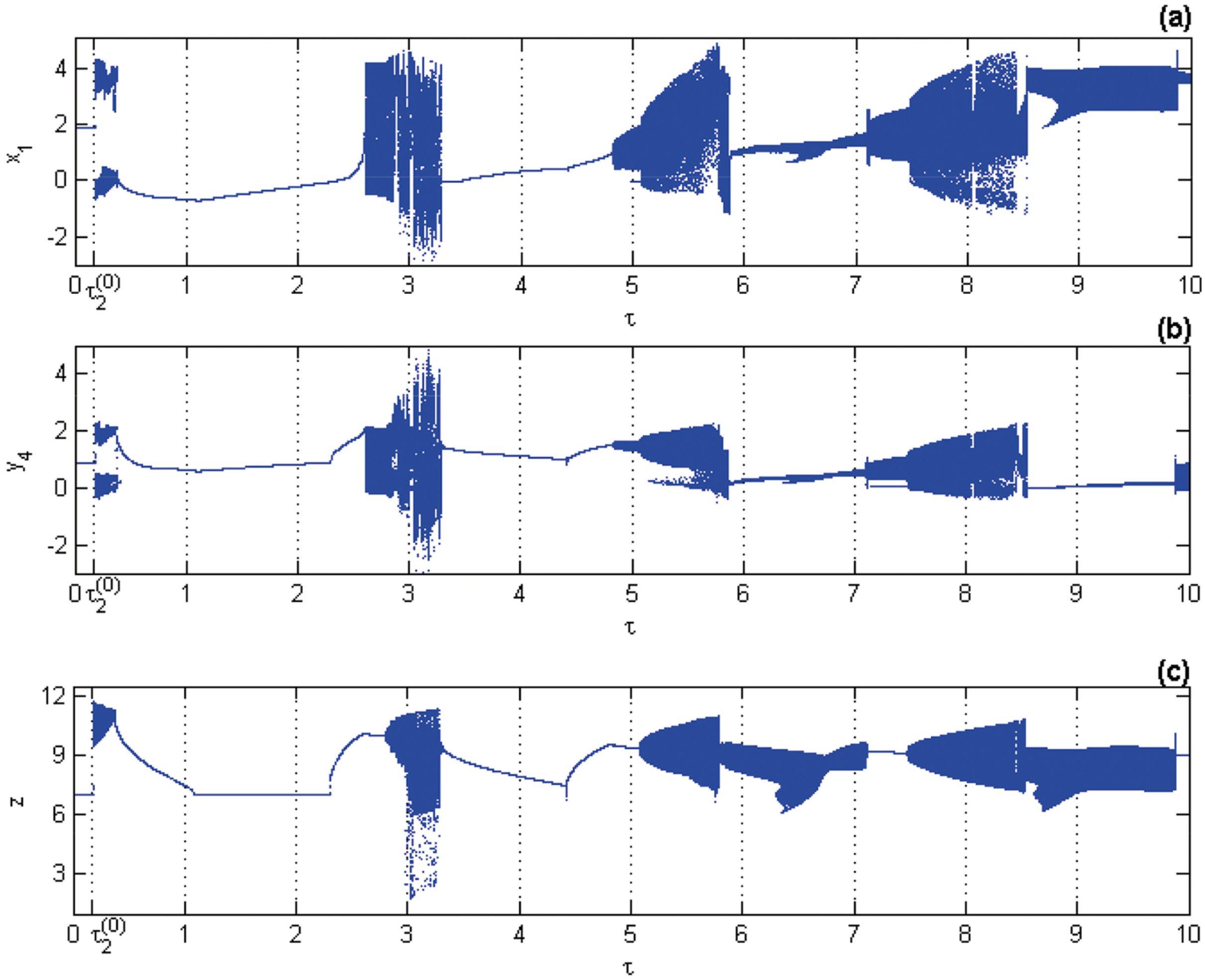

Fig. 8. Bifurcation diagrams of time delay system (4) for the parameters values $\sigma = 6$, $\beta = 1$, $n = 5$, $\rho = 8$. (a) $x_1(t)$ *versus* τ. (b) $y_4(t)$ *versus* τ. (c) $z(t)$ *versus* τ.

5 Lyapunov exponents and Kolmogorov-Sinai entropy of (4)

In this section, the Lyapunov exponents and Kolmogorov-Sinai (KS) entropy of system (4) utilized for the choice $\sigma = 15$, $\beta = \frac{8}{3}$, $\rho = 28$ and different values of τ and n are computed. The values of τ at which chaotic, hyperchaotic solutions as well as solutions that approach fixed points are calculated. Other choices of the system parameters and n can be similarly studied. Using the methods provided by Breda and Van Vleck [26], the Lyapunov exponents are calculated.

Another sign that measures the complexity and the dynamics of system (4) is the KS entropy, that equals to the sum of all the positive Lyapunov exponents [27,28],

$$h_{KS} = \sum_{r=1}^{k} \lambda_r,$$
$$\lambda_r > 0\,(r = 1, 2, \ldots, k)\,, \lambda_{k+1} \leq 0, \tag{55}$$

where the Lyapunov exponents are ordered as $\lambda_r \geq \lambda_{r+1}$ and h_{KS} is positive for chaotic and hyperchaotic solutions and zero for periodic attractors or solutions that approach fixed points. Different values of n are considered below.

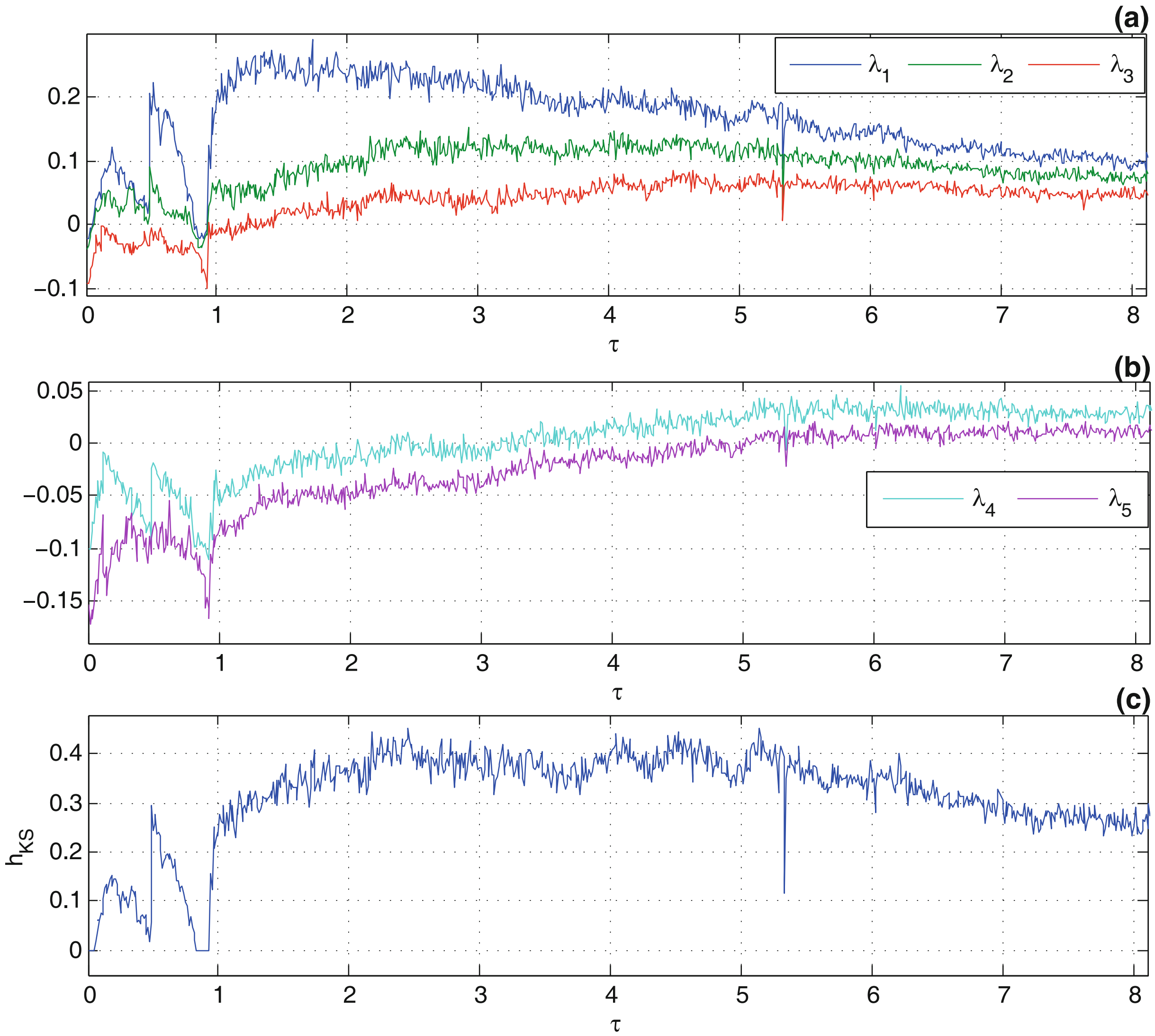

Fig. 9. Lyapunov exponents of (4) *versus* τ and the correspondence KS entropy, when $\sigma = 15$, $\beta = \frac{8}{3}$, $\rho = 28$, $n = 2$. (a) λ_1, λ_2, λ_3 *versus* τ. (b) λ_4, λ_5 *versus* τ. (c) KS entropy.

5.1 The case n = 2

For this case, the Lyapunov exponents $\lambda_1, \ldots, \lambda_5$ *versus* τ are calculated as shown in fig. 9(a), (b). It is concluded that system (4) has hyperchaotic attractors of order 5 for $\tau \in [5.03, 5.04], [5.07, 5.63]$ and $[5.66, 8]$, while the hyperchaotic attractors of order 4 exist for τ lies in the intervals $[2.32, 2.33]$, $[2.4, 2.45]$, $[3.16, 3.2]$, $[3.23, 3.25]$, $[3.29, 3.32]$, $[3.35, 5.02]$, $[5.05, 5.06]$ and $[5.64, 5.65]$. It also has a hyperchaotic attractor of order 3 for $\tau \in [1.33, 1.39]$, $[1.44, 2.31]$, $[2.34, 2.39]$, $[2.46, 3.15]$, $[3.21, 3.22]$, $[3.26, 3.28]$, $[3.33, 3.34]$, hyperchaotic attractor of order 2 for $\tau \in [0.06, 0.8]$, $[0.95, 1.32]$ and $[1.4, 1.43]$. The chaotic attractors are found for $\tau \in [0.81, 0.82] \cup [3.3, 3.5]$. The attractors of system (4) that approach trivial fixed points are exist for $\tau \in (0, 0.05] \cup [0.83, 0.93]$. The KS entropy is simulated in fig. 9(c). It is clear that the dynamics of this system is complex and rich since it has chaotic and hyperchaotic attractors of different orders for large and small intervals of τ. Additionally, $h_{KS} = 0$ for $\tau \in (0, 0.05] \cup [0.83, 0.93]$ and positive for chaotic and hyperchaotic attractors.

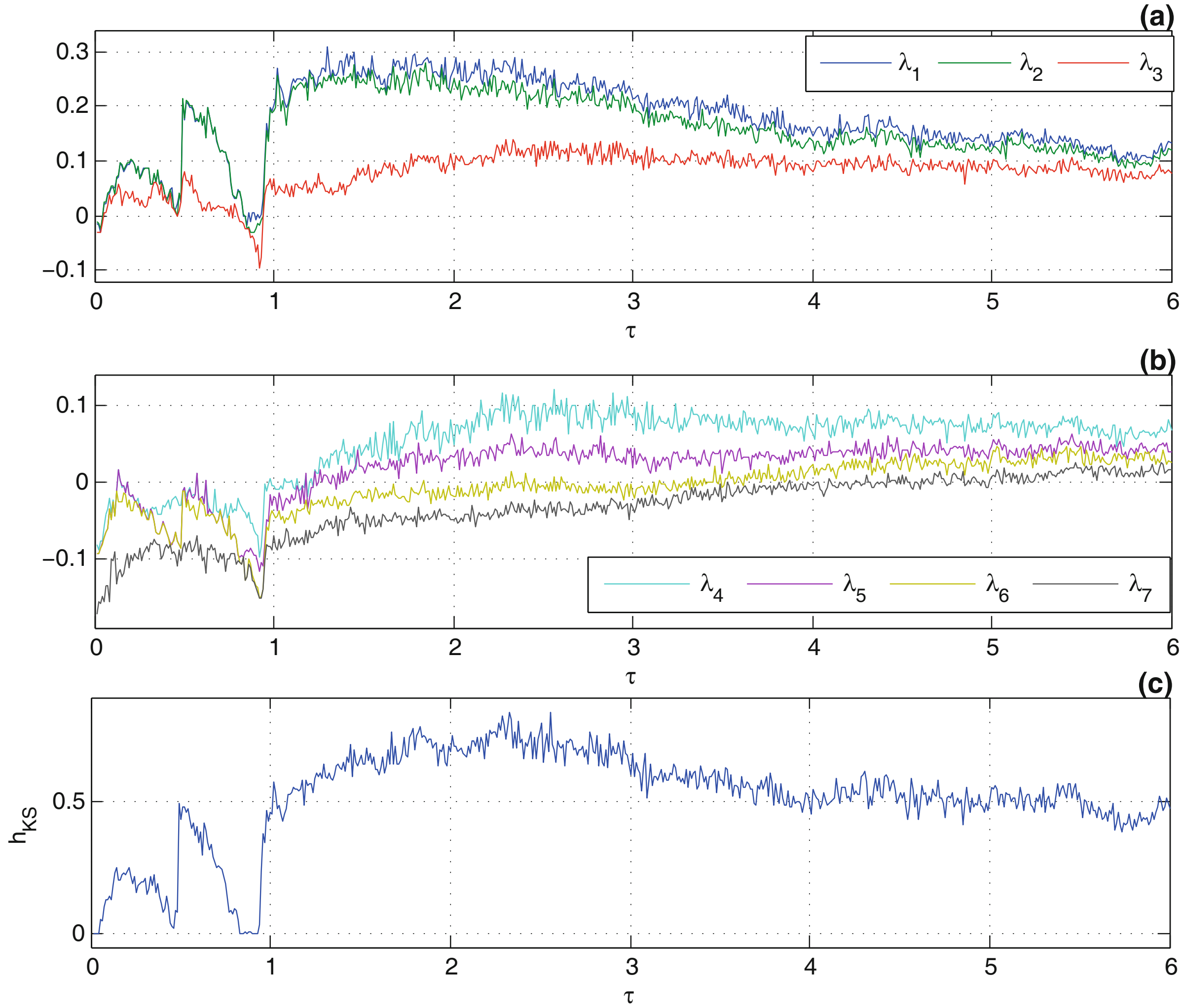

Fig. 10. Lyapunov exponents of (4) *versus* τ and the correspondence KS entropy, when $\sigma = 15$, $\beta = \frac{8}{3}$, $\rho = 28$, $n = 3$. (a) λ_1, λ_2, λ_3 *versus* τ. (b) λ_4, λ_5, λ_6, λ_7 *versus* τ. (c) KS entropy.

5.2 The case $n = 3$

As we did in subsect. 5.1, we calculated λ_k $(k = 1, 2, \ldots, 7)$ *versus* τ and they are plotted in fig. 10(a), (b). The hyperchaotic attractors of order 7 exist for τ lies in the intervals $[4.42, 4.52]$, $[4.63, 4.64]$, $[4.68, 4.73]$, $[4.78, 4.84]$, $[4.89, 4.91]$, $[4.99, 5.21]$ and $[5.24, 6]$ while the hyperchaotic attractors of order 6 exist for $\tau \in [2.32, 2.33]$, $[3.52, 3.56]$, $[3.59, 3.6]$, $[3.63, 4.41]$, $[4.53, 4.62]$, $[4.65, 4.67]$, $[4.74, 4.77]$ and $[4.85, 4.88]$. This system has hyperchaotic attractors of order 5 for $\tau \in (0.12, 0.14]$, $[1.28, 1.3]$, $[1.33, 2.31]$, $[2.34, 3.51]$, $[3.57, 3.58]$ and $[3.61, 3.62]$, hyperchaotic attractors of order 4 for $\tau \in [1.2, 1.27]$, $[1.31, 1.32]$, hyperchaotic of order 3 for $\tau \in [0.05, 0.12]$, $(0.14, 0.79]$, $(0.94, 1.2)$, hyperchaotic attractors of order 2 for $\tau \in (0.79, 0.84)$, chaotic attractor for $\tau \in (0.87, 0.94]$. It has solutions that approach trivial fixed points for $\tau \in (0, 0.05) \cup [0.84, 0.87]$. The KS entropy is plotted in fig. 10(c). It is concluded that the dynamics of this system are rich and complex.

5.3 The case $n = 10$

In this case system (4) with $n = 10$ has 21 Lyapunov exponents and hyperchaotic attractors of order 21 for $\tau \in [3.99, 4.01]$, $[4.06.4.09]$. It has, also, chaotic and hyperchaotic attractors of orders $20, 19, \ldots, 2$ for different values of τ. In fig. 11, the KS entropy is depicted and observed for $\tau \in (0, 0.05] \cup [0.83, 0.93]$ that $h_{KS} = 0$. The dynamics of this system in this case are similar to those cases for $n = 2, 3$.

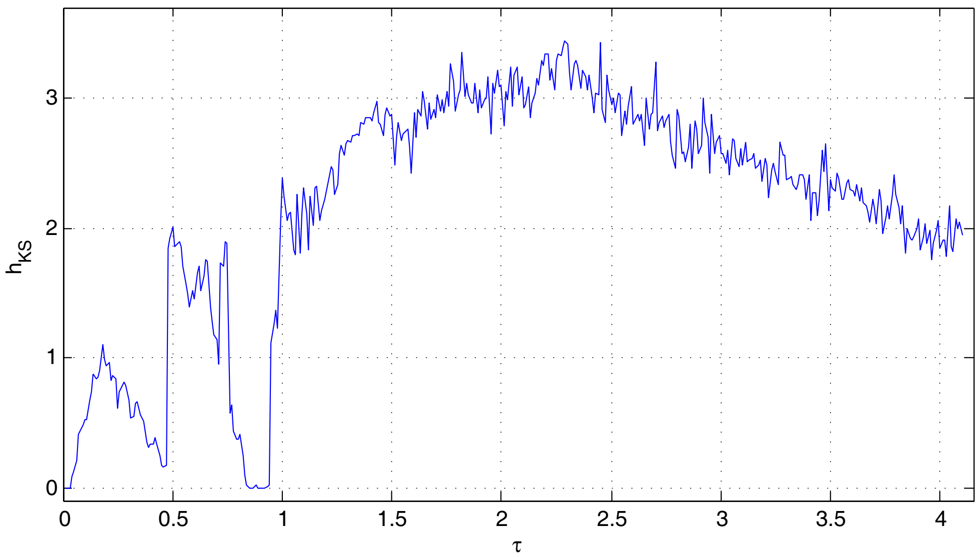

Fig. 11. The KS entropy for system (4) *versus* τ, when $\sigma = 15$, $\beta = \frac{8}{3}$, $\rho = 28$, $n = 10$.

6 Conclusions

This paper deals with nonlinear models, in which some variables have n dimension, since they are related to networks applications and secure communications. In this paper, a generalized Lorenz system of $(2n+1)$ dimension with time delay has been introduced and studied. Namely, by taking the state variables x and $y \in \mathbb{R}^n$. As seen from remarks 1 and 2, the new system (4) is a generalization of Lorenz system (1) and complex Lorenz system (3) by setting $n = 1$ and $n = 2$, respectively. Moreover, this system may belong to Clifford algebra. The complex dynamical behaviors of system (4) are studied in detail. It has one trivial and two nontrivial fixed points, which are generalizations of the fixed points of Lorenz system [1] and complex Lorenz system [7]. By analyzing the distribution of the eigenvalues of the transcendental characteristic equation of the corresponding linearized system, local stability criteria are achieved, see theorems 1 and 2. By choosing time delay as a bifurcation parameter, the model is found to undergo a sequence of Hopf bifurcation when this parameter passes through a critical value τ_0 as in eqs. (18) and (30). Furthermore, by using the center manifold theorem and the normal form theory, the direction and the stability of the bifurcating periodic solutions are determined in sect. 3. That is, a class of periodic orbits bifurcates from the corresponding fixed points and the bifurcation diagrams are shown in figs. 5 and 8. Furthermore, we simulated the bifurcation diagrams for both cases of the stability of trivial and nontrivial fixed points to bring out the nature of the underlying dynamics, see figs. 5 and 8. Finally, by varying the τ parameter, chaotic and hyperchaotic attractors of order $(2n+1)$ exist. The values of τ are calculated numerically for $n = 2, 3, 10$. Moreover, we plotted the KS entropy of system (4) for $n = 2, 3$, and 10 in figs. 9(c), 10(c) and 11, respectively.

Interestingly, there are some properties of the time delay Lorenz system (4). For instance, the existence of delay in the system, infinite dimensionality of delayed systems offers a great opportunity to the researchers to investigate hyperchaos (two or more than two positive Lyapunov exponents). The complex Lorenz system (3) has one positive Lyapunov exponent [7], but this system with delay has 5 positive Lyapunov exponents, as shown in fig. 9(a), (b). To conclude for the parameters $\sigma = 15$, $\beta = \frac{8}{3}$, $\rho = 28$, the time delay Lorenz system (4) with dimension $(2n+1)$ has $(2n+1)$ positive Lyapunov exponents for some values of τ. Moreover, the time delay system (3) has infinite number of eigenvalues, because of the exponential in the characteristic equations (7) and (23), while systems (1) and (3) have only three and five eigenvalues, respectively. Therefore, the results of this work can be considered as a generalization of those results in the literature. It is reckoned that this system will have broad applications in networks, engineering systems and secure communications. Our system (4) leaves room for further investigations, *e.g.* the boundedness of solutions which it is important in control theory and its applications, basin of attractions, and instead of constant delay one can consider the time varying delay.

We would like to thank Prof. Dimitri Breda, assistant professor at University of Udine, for providing the scripts used to calculate the Lyapunov exponents.

References

1. E.N. Lorenz, J. Atmos. Sci. **20**, 130 (1963).
2. G. Chen, T. Ueta, Int. J. Bifurc. Chaos **9**, 1465 (1999).
3. O.E. Rössler, Phys. Lett. A **57**, 397 (1976).
4. J. Lü, G. Chen, S. Zhang, Chaos Solitons Fractals **14**, 669 (2002).
5. L.O. Chua, M. Komuro, T. Matsumoto, IEEE Trans. Circuits Syst. **33**, 1072 (1986).
6. A.C. Fowler, M.J. McGuinness, J.D. Gibbon, Physica D **4**, 139 (1982).
7. G.M. Mahmoud, M.A. Al-Kashif, S.A. Aly, Int. J. Mod. Phys. C **18**, 253 (2007).
8. L. Cveticanin, Mech. Mach. Theory **30**, 581 (1995).
9. C.Z. Ning, H. Haken, Phys. Rev. A **41**, 3826 (1990).
10. A.C. Newell, J.V. Moloney, *Nonlinear Optics* (Addison-Wesley, 1992).
11. H. Richter, Chaos Solitons Fractals **12**, 2375 (2001).
12. S.I. Niculescu, *Delay Effects on Stability: A Robust Control Approach* (Springer, Heidelberg, 2001).
13. N. MacDonald, *Biological Delay Systems: Linear Stability Theory* (Cambridge University Press, Cambridge, 1989).
14. Y. Kuang, *Delay Differential Equations with Applications in Population Dynamics* (Academic Press, Boston, 1993).
15. M.C. Mackey, L. Glass, Science **197**, 287 (1977).
16. K. Ikeda, Opt. Commun. **30**, 257 (1979).
17. D. Ghosh, R. Chowdhury, P. Saha, Chaos Solitons Fractals **35**, 472 (2008).
18. A. Sharma, M.D. Shrimali, A. Prasad, R. Ramaswamy, Eur. Phys. J. ST **226**, 1903 (2017).
19. T. Banerjee, D. Biswas, B.C. Sarkar, Nonlinear Dyn. **70**, 721 (2012).
20. G.M. Mahmoud, E.E. Mahmoud, A.A. Arafa, Nonlinear Dyn. **80**, 855 (2015).
21. R. Jaimes-Reátegui *et al.*, Eur. Phys. J. ST **225**, 2707 (2016).
22. Z. Wang, W. Sun, Z. Wei, S. Zhang, Nonlinear Dyn. **82**, 577 (2015).
23. V.-T. Pham *et al.*, Eur. Phys. J. ST **225**, 127 (2016).
24. B. Hassard, N. Kazarinoff, Y. Wan, *Theory and Applications of Hopf Bifurcation* (Cambridge University Press, Cambridge, 1981).
25. Y. Song, J. Wei, Chaos Solitons Fractals **22**, 75 (2004).
26. D. Breda, E. Van Vleck, Numer. Math. **126**, 225 (2013).
27. R. Vicente, J. Daudén, P. Colet, R. Toral, IEEE J. Quantum Elect. **41**, 541 (2005).
28. A. Uchida, *Optical Communication with Chaotic Lasers: Applications of Nonlinear Dynamics and Synchronization* (John Wiley & Sons, 2012).